Autonomic Neuroscience: Basic and Clinical

Exploring mean square prediction error and correlation metrics for the computation of the autoregulation index during propofol-based general anesthesia and head-up tilt protocols

--Manuscript Draft--

Manuscript Number:	
Article Type:	VSI: ANS-CA
Section/Category:	Clinical autonomic neuroscience
Keywords:	Spontaneous variability; cerebral autoregulation; head-up tilt; propofol general anesthesia; cerebrovascular control; autonomic nervous system
Corresponding Author:	Alberto Porta, Ph.D. Università degli Studi di Milano: Universita degli Studi di Milano San Donato Milanese, Milan, Lombardia ITALY
First Author:	Vlasta Bari
Order of Authors:	Vlasta Bari
	Lorenzo Barbarossa
	Francesca Gelpi
	Beatrice Cairo
	Beatrice De Maria
	Davide Tonon
	Gianluca Rossato
	Luca Faes
	Marco Ranucci
	Riccardo Barbieri
	Alberto Porta, Ph.D.
Abstract:	Cerebral autoregulation (CA) is evaluated via the autoregulation index (ARI) derived from several techniques grounded on the simultaneous utilization of Tiecks' differential equations and spontaneous variability of mean arterial pressure (MAP) and mean cerebral blood flow velocity (MCBFV) recorded from middle cerebral arteries through a transcranial Doppler device. These techniques exploit two metrics for comparing the measured, or data-driven, MCBFV series with the version predicted by Tiecks' model: normalized mean square prediction error (NMSPE) and normalized correlation ρ. The two metrics for ARI computation were tested in 13 healthy subjects (age: 27±8 yrs, 5 males) at rest in supine position (REST) and during 60° head-up tilt (HUT) and in 19 patients (age: 64±8 yrs, all males), scheduled for coronary artery bypass grafting, before (PRE) and after (POST) propofol-based general anesthesia induction. Analyses were carried out over matched original MAP and MCBFV pairs and surrogate unmatched couples taken from different subjects within the same group and condition. We found that: i) both NMSPE and ρ metrics were appropriate for ARI evaluation in the REST-HUT protocol; ii) ρ metric was preferable to NMSPE for its better ability to separate original from surrogate pairs in the PRE-POST protocol; iii) the two metrics led to similar ARIs; iv) CA was not different during HUT or POST compared to baseline condition and this conclusion held regardless of the technique and metric for ARI estimation. We recommend the use of ρ for ARI estimation.
Suggested Reviewers:	Yu-Chieh Tzeng University of Otago Wellington shieak.tzeng@otago.ac.nz Wide experience in biomedical signal processing and assessment of cerebrovascular control

	Ronney Panerai University of Leicester rp9@le.ac.uk Wide experience in biomedical signal processing and assessment of cerebral autoregulation
	David Simpson University of Southampton ds@isvr.soton.ac.uk Wide experience in biomedical signal processing and assessment of cerebral autoregulation
	Mathias Baumert University of Adelaide mathias.baumert@adelaide.edu.au Wide experience in biomedical signal processing and time series analysis
	Michal Javorka Comenius University Michal.Javorka@jfmed.uniba.sk Relevant experience in interpreting physiological variability
Opposed Reviewers:	

Dear Editor,

Please find our manuscript entitled “Exploring mean square prediction error and correlation metrics for the computation of the autoregulation index during propofol-based general anesthesia and head-up tilt protocols” by Vlasta Bari, Lorenzo Barbarossa, Francesca Gelpi, Beatrice Cairo, Beatrice De Maria, Davide Tonon, Gianluca Rossato, Luca Faes, Marco Ranucci, Riccardo Barbieri, Alberto Porta, which we are submitting for consideration in Autonomic Neuroscience: Basic and Clinical.

The manuscript is here submitted for evaluating its suitability to be included in the Special Issue “Autonomic nervous system and cerebral blood flow autoregulation”. Guest Editors: Alberto Porta and Ronney Panerai.

The study originally tests two metrics commonly utilized for comparing the measured, or data-driven, mean cerebral blood flow velocity (MCBFV) series with the version predicted by Tiecks’ model, namely normalized mean square prediction error (NMSPE) and normalized correlation ρ, in the context of the assessment of the autoregulation index (ARI) from spontaneous variability of mean arterial pressure (MAP) and MCBFV.

The study was carried out in a group of healthy subjects during head-up tilt and in subjects scheduled for coronary artery bypass grafting during propofol-based general anesthesia.

From a methodological standpoint we found that NMSPE and ρ metrics were appropriate for ARI evaluation in response to postural challenge, while ρ metric was preferable to NMSPE for its better ability to separate original from surrogate pairs during propofol-based general anesthesia.

From an experimental standpoint we found that the estimated ARIs were similar during orthostatic challenge compared to supine position and during propofol-based general anesthesia compared to baseline condition and this conclusion held regardless of the technique and metric for ARI estimation.

Given the better performance during propofol-based general anesthesia protocol we recommend the use of ρ with respect to NMSPE when assessing ARI via the application of methods exploiting Tiecks’ model.

The present manuscript has not been published and is not being considered for publication elsewhere. All authors have taken due care to ensure the integrity of the work, meet criteria for authorship, all those who qualify for authorship have been listed, and have seen and approved the manuscript.

Sincerely yours,

Alberto Porta

Highlights

1) Two metrics for assessing autoregulation index (ARI) from spontaneous variations are tested
2) Correlation metric is more powerful than mean square prediction error
3) ARIs estimated by the two metrics are similar
4) Head-up tilt and propofol-based general anesthesia do not affect cerebral autoregulation
5) This conclusion holds regardless of metric utilized for ARI estimation

Cerebral autoregulation during general anesthesia and postural challenge by V. Bari et al.

Abstract

Cerebral autoregulation (CA) is evaluated via the autoregulation index (ARI) derived from several techniques grounded on the simultaneous utilization of Tiecks' differential equations and spontaneous variability of mean arterial pressure (MAP) and mean cerebral blood flow velocity (MCBFV) recorded from middle cerebral arteries through a transcranial Doppler device. These techniques exploit two metrics for comparing the measured, or data-driven, MCBFV series with the version predicted by Tiecks' model: normalized mean square prediction error (NMSPE) and normalized correlation ρ. The two metrics for ARI computation were tested in 13 healthy subjects (age: 27±8 yrs, 5 males) at rest in supine position (REST) and during 60° head-up tilt (HUT) and in 19 patients (age: 64±8 yrs, all males), scheduled for coronary artery bypass grafting, before (PRE) and after (POST) propofol-based general anesthesia induction. Analyses were carried out over matched original MAP and MCBFV pairs and surrogate unmatched couples taken from different subjects within the same group and condition. We found that: i) both NMSPE and ρ metrics were appropriate for ARI evaluation in the REST-HUT protocol; ii) ρ metric was preferable to NMSPE for its better ability to separate original from surrogate pairs in the PRE-POST protocol; iii) the two metrics led to similar ARIs; iv) CA was not different during HUT or POST compared to baseline condition and this conclusion held regardless of the technique and metric for ARI estimation. We recommend the use of ρ for ARI estimation.

Exploring mean square prediction error and correlation metrics for the computation of the autoregulation index during propofol-based general anesthesia and head-up tilt protocols

Vlasta Bari[1], Lorenzo Barbarossa[2], Francesca Gelpi[1,3], Beatrice Cairo[3], Beatrice De Maria[4], Davide Tonon[5], Gianluca Rossato[5], Luca Faes[6], Marco Ranucci[1], Riccardo Barbieri[2], Alberto Porta[1,3]

[1]Department of Cardiothoracic, Vascular Anesthesia and Intensive Care, IRCCS Policlinico San Donato, San Donato Milanese, Milan, Italy
[2]Department of Electronics Information and Bioengineering, Politecnico di Milano, Milan, Italy
[3]Department of Biomedical Sciences for Health, University of Milan, Milan, Italy
[4]IRCCS Istituti Clinici Scientifici Maugeri, Milan, Italy
[5]Department of Neurology, IRCCS Sacro Cuore Don Calabria Hospital, Negrar, Verona, Italy
[6]Department of Engineering, University of Palermo, Palermo, Italy

Running title: Cerebral autoregulation during general anesthesia and postural challenge

Address for correspondence:

Prof. Alberto Porta, PhD
Università degli Studi di Milano
Dipartimento di Scienze Biomediche per la Salute
IRCCS Policlinico San Donato
Laboratorio di Modellistica di Sistemi Complessi
Via R. Morandi 30
20097, San Donato Milanese
Milano, Italy

Tel: +39 02 52774382
Email: alberto.porta@unimi.it

Abstract

Cerebral autoregulation (CA) is evaluated via the autoregulation index (ARI) derived from several techniques grounded on the simultaneous utilization of Tiecks' differential equations and spontaneous variability of mean arterial pressure (MAP) and mean cerebral blood flow velocity (MCBFV) recorded from middle cerebral arteries through a transcranial Doppler device. These techniques exploit two metrics for comparing the measured, or data-driven, MCBFV series with the version predicted by Tiecks' model: normalized mean square prediction error (NMSPE) and normalized correlation ρ. The two metrics for ARI computation were tested in 13 healthy subjects (age: 27±8 yrs, 5 males) at rest in supine position (REST) and during 60° head-up tilt (HUT) and in 19 patients (age: 64±8 yrs, all males), scheduled for coronary artery bypass grafting, before (PRE) and after (POST) propofol-based general anesthesia induction. Analyses were carried out over matched original MAP and MCBFV pairs and surrogate unmatched couples taken from different subjects within the same group and condition. We found that: i) both NMSPE and ρ metrics were appropriate for ARI evaluation in the REST-HUT protocol; ii) ρ metric was preferable to NMSPE for its better ability to separate original from surrogate pairs in the PRE-POST protocol; iii) the two metrics led to similar ARIs; iv) CA was not different during HUT or POST compared to baseline condition and this conclusion held regardless of the technique and metric for ARI estimation. We recommend the use of ρ for ARI estimation.

Keywords: Spontaneous variability; cerebral autoregulation; head-up tilt; propofol general anesthesia; cerebrovascular control; autonomic nervous system.

Highlights

1) Two metrics for assessing autoregulation index (ARI) from spontaneous variations are tested
2) Correlation metric is more powerful than mean square prediction error
3) ARIs estimated by the two metrics are similar
4) Head-up tilt and propofol-based general anesthesia do not affect cerebral autoregulation
5) This conclusion holds regardless of metric utilized for ARI estimation

1. Introduction

Variability of the mean cerebral blood flow (MCBF) is deemed to be detrimental for brain perfusion and, as such, the amplitude of the MCBF fluctuations is to be reduced. Cerebral autoregulation (CA) is a physiological mechanism responsible to keep MCBF unvaried and limit its variability in presence of changes of mean arterial pressure (MAP) (Aaslid et al., 1989; Paulson et al., 1990). MCBF velocity, (MCBFV), derived via transcranial Doppler device, is generally utilized as a surrogate of MCBF (Aaslid et al., 1982), while changes in MAP are generally assessed from systemic arterial pressure under the hypothesis that intracranial pressure does not vary. CA can be studied by either static (Paulson et al., 1990; Strandgaard and Paulson, 1984; Lassen, 1959) or dynamic (Newell et al., 1994; Aaslid et al., 1989; Panerai et al., 1998; Czosnyka et al., 2008) methods, with the latter exploiting MAP changes induced by an external intervention, e.g. thigh cuff deflation, or MAP variations occurring spontaneously due to the action of cardiovascular control mechanisms (Penzel et al., 2017).

There is a considerable interest in testing whether CA is working based on spontaneous variability of MAP and MCBFV (Panerai et al., 2001; Carey et al., 2001; Castro et al., 2014; Claassen et al., 2016; Dineen et al., 2010; Lee et al., 2020). A remarkable set of methods applied to MAP and MCBFV variability to grade CA (Panerai et al., 1998; Panerai et al., 1999; Simpson et al., 2001; Panerai et al., 2003; Mahdi et al., 2017) is grounded on Tiecks' model devised to describe the response of MCBFV to a sudden and sustained change in MAP (Tiecks et al., 1995). These methods can be roughly classified into: i) the time domain method (TDM) that feeds the Tiecks' differential equations with spontaneous MAP variability to observe the evolution of MCBFV and compares the predicted MCBFV variability series with the recorded one (Panerai et al., 2003; Mahdi et al., 2017); ii) the nonparametric method (nonPM) grounded on Fourier transform-based estimation of the MCBFV-MAP transfer function, the assessment of its impulse response (IR), or step response (SR), and the comparison of the IR, or SR, to that of Tiecks' model (Panerai et al., 1998; Panerai et al., 1999); iii) the parametric method (PM) based on estimation of a MCBFV-MAP dynamical model, mainly belonging to the linear or nonlinear vector regression class, the computation of its IR, or SR, and the comparison of the IR, or SR, to that derived from Tiecks' differential equations (Panerai et al., 1999; Simpson et al., 2001; Gelpi et al., 2021). Tiecks' model can be graded according to the type of the MCBFV response to a sustained drop of MAP and this grading, identified by a parameter referred to as autoregulation index (ARI), is ranked from 0 to 9, where ARIs smaller than, or equal to 4, indicate impaired CA and ARIs greater than 4 indicate a working CA (Tiecks et al., 1995).

Regardless of the technique exploited for ARI estimation (i.e. TDM, nonPM or PM), the comparison between the measured, or data-driven, MCBFV series and the version predicted by

Tiecks' differential equations is performed through a figure of merit estimating the degree of similarity between them. The most frequently utilized metric is the normalized mean square prediction error (NMSPE) (Angarita-Jaimes et al., 2014): the closer to 0 the NMSPE, the more adequate the Tiecks' model in describing the measured MCBFV dynamics. In order to overcome limitations linked to the possible presence of subjects in which the magnitude of the absolute prediction error might exhibit important deviations due to the presence of constant biases in the procedure of measurement, some studies have suggested the use of the normalized correlation ρ between the measured and the predicted MCBFV series to assess their level of agreement (Dawson et al., 2000): the closer to 1 the ρ, the better the description of the measured MCBFV dynamics provided by Tiecks' model. However, these two metrics were never systematically tested, thus preventing a ranking in practical settings and to understand whether conclusions of the study might depend on the selection of the figure of merit.

Thus, the aim of this study was to compare NMSPE and ρ metrics for the ARI computation in two experimental protocols applying two different challenges to CA, namely a gravitational challenge, and the typical challenge occurring just before major surgical interventions, namely general anesthesia. In healthy subjects, in spite of a sympathetic activation provoking peripheral vasoconstriction favoring venous return (Montano et al., 1994; Cooke et al., 1999; Furlan et al., 2000; Marchi et al., 2016), an orthostatic challenge did not affect CA (Carey et al., 2001; Schondorf et al., 2001; Castro et al., 2017; Claydon and Hainsworth, 2003; Bari et al., 2017; Gelpi et al., 2021). Propofol-based general anesthesia is known to preserve CA (Strebel et al., 1995; Engelhard et al., 2001; Ogawa et al., 2010) in a context of depressed autonomic function, especially sympathetic control (Ebert et al., 1992; Sellgren et al., 1994; Boer et al., 1990), reduced baroreflex sensitivity (Keyl et al., 2000; Sato et al., 2005; Porta et al., 2013, Bari et al., 2019), and weakened association between MCBFV and MAP (Bari et al., 2021). The present study aims at checking whether these conclusions might depend on the metrics utilized for ARI calculation.

2. Methods

2.1 ARI approaches

ARI was assessed according to techniques exploiting simultaneously the modeling approach originally developed by Tiecks et al., (1995) to describe CA in the context of the interventional procedure of thigh cuff deflation (Aaslid et al., 1989) and MAP and MCBFV spontaneous variabilities. The Tiecks' model describes the dynamical link from MAP to MCBFV as a derivative filter and allows the computation of the response to the original MCBFV series or, in alternative the IR, or the SR, of the model. These responses are graded according to integer values of an

autoregulation index (ARI) ranking the efficiency in performing CA from 0, i.e., absent CA, to 9, i.e., excellent CA with ARI values smaller than, or equal to, 4 indicating an impaired CA and those greater than 4 a working CA (Tiecks et al., 1995). The response derived from Tiecks' model was compared to those obtained from spontaneous variations of MAP and MCBFV as a function of ARI with the aim at selecting the response that provides the best agreement with real data and storing the correspondent ARI. We considered four approaches to the ARI estimation: i) the TDM in which the Tiecks' model was driven by the original MAP variability to derive the corresponding MCBFV series that was compared with the original MCBFV variability (Panerai et al., 2003; Mahdi et al., 2017); ii) the non-PM based on the SR in which the SR of the Tiecks' model was compared to the one derived from the MCBFV-MAP transfer function estimated via a non-PM technique (Panerai et al., 1998; Panerai et al., 1999); iii) the PM method based on the IR in which the IR of the Tiecks' model was compared to the one derived from model-based approach exploiting a PM technique (Panerai et al., 1999; Simpson et al., 2001; Gelpi et al., 2021); iv) the PM based on the SR in which the SR of the Tiecks' model was compared to the one derived from model-based approach exploiting a PM technique (Panerai et al., 1999; Simpson et al., 2001; Gelpi et al., 2021). The exclusion of the non-PM based on the IR is due to its limited efficiency in presence of noise as proven in (Gelpi et al., 2021). We referred to (Gelpi et al., 2021) for a deep description of all the implemented ARI approaches and to the original papers where the methods are first described (Panerai et al., 1998; Panerai et al., 1999; Simpson et al., 2001; Panerai et al., 2003; Mahdi et al., 2017).

2.2 Figures of merit for ARI assessment

The comparison between measured, or data-driven, and model-predicted MCBFV curves was performed according to two different metrics. The first metric is the NMSPE (Angarita-Jaimes et al., 2014). The NMSPE was computed as the mean square value of the difference between the measured and predicted MCBFV series normalized by the mean square value of the measured MCBFV. The NMSPE was calculated for the ten different ARI curves. We selected the ARI (i.e. from 0 to 9) corresponding to the minimum value of NMSPE. The second metric is the correlation ρ between the measured and the predicted MCBFV computed as their cross-correlation at 0 lag (Dawson et al., 2000; Porta et al., 2007a). In the TDM measured and predicted MCBFV were normalized to have zero mean and unit variance by subtracting the mean and dividing each variation from the mean by the standard deviation. In PM and nonPM the series were normalized according to the strategy described in (Gelpi et al., 2021). ρ was calculated for the ten different ARI curves. We selected the ARI (i.e. from 0 to 9) corresponding to the maximum value of ρ. Since no interpolation procedure was made, ARI estimated via both NMSPE and ρ assumed only integer values. NMSPE and ρ were

calculated for each of the four different methods for ARI estimation. The metrics were labelled $NMSPE_{TDM}$, $NMSPE_{nonPM,SR}$, $NMSPE_{PM,IR}$, $NMSPE_{PM,SR}$, ρ_{TDM}, $\rho_{nonPM,SR}$, $\rho_{PM,IR}$ and $\rho_{PM,SR}$, while the corresponding optimized ARI were labeled as ARI_{TDM}, $ARI_{,nonPM,SR}$, $ARI_{PM,IR}$ and $ARI_{,PM,SR}$.

2.3 Surrogate analysis

Surrogate pairs have been created to test the significance of metrics utilized to compare original and predicted MCBFV series. Surrogate couples were built by randomly associating MAP series of one subject to the MCBFV series derived from another subject within the same protocol and experimental condition (Van Leeuwen et al., 2003; Panerai et al, 2018). NMSPE and ρ were calculated over both original and surrogate pairs. NMSPE is expected to be higher in surrogates than in original time series because a random association would lead to a higher error in predicting MCBFV. On the contrary, ρ is expected to be lower in surrogates than in original series, because a random association would lead to a lower correlation between the original and predicted series.

3. Experimental protocols and data analysis

3.1 Ethics

The metrics for testing similarity between original and predicted MCBFV fluctuations were tested in two different experimental protocols carried out, respectively, in a group of healthy subjects undergoing recordings at rest in supine position (REST) and during postural challenge induced by head-up tilt (HUT) (Faes et al. 2013; Bari et al., 2016) and in a group of individuals, scheduled for coronary artery bypass grafting, undergoing recordings before (PRE) and after (POST) propofol-based general anesthesia induction (Bari et al., 2021). Data of the REST-HUT experimental protocol were collected the Neurology Division of Sacro Cuore Hospital, Negrar, Italy. The inclusion criteria, ethical committee approval from Sacro Cuore Hospital, Negrar, Italy (approval number: 101/2010), agreement with the principles of the Declaration of Helsinki and informed consent process were described in (Faes et al. 2013; Bari et al., 2016). Data of the PRE-POST experimental protocol were collected at the Department of Cardiothoracic, Vascular Anesthesia and Intensive Care of IRCCS Policlinico San Donato, San Donato Milanese, Milan, Italy. The inclusion criteria, ethical committee approval from San Raffaele Hospital, Milan, Italy (approval number: 40/int/2016), agreement with the principles of the Declaration of Helsinki and informed consent process were described in (Bari et al., 2021).

3.2 REST-HUT experimental protocol

Details of the REST-HUT experimental protocol can be found in (Faes et al. 2013; Bari et al., 2016). Briefly, we enrolled 13 healthy subjects (age: 27±8 yrs, 5 males). None of subjects experienced events of syncope in the previous 2 years and were taking any medication affecting cardiovascular control. The healthy status of the subjects was confirmed via physical and full neurological assessment. We acquired electrocardiogram (ECG) from lead II, arterial pressure (AP) via a volume-clamp device from the middle finger of the right hand (Finapres Medical Systems, Enschede, The Netherlands) and cerebral blood flow velocity (CBFV) from the middle cerebral artery through a transcranial Doppler device (Multi-Dop T, DWL, 2MHz, Compumedics, San Juan Capistrano, CA, USA). Sampling frequency was set to 1000 Hz. The CBFV was low-pass filtered with cut-off frequency of 10 Hz. Subjects were instructed to avoid caffeinated and alcoholic beverages for 24h before the study. Experiments took place in the morning in a temperature-controlled room. After having instrumented the subject, a period of 5 minutes was left for stabilization of the physiological variables. Then, the subjects underwent recordings for 10 minutes at REST followed by HUT with tilt table inclination of 60°. None of the subjects exhibited presyncope signs during HUT. Signals were analyzed within the first 10 minutes after the onset of HUT. The first three minutes of HUT session were discarded to avoid transitory adjustments of the variables.

3.3 PRE-POST experimental protocol

Details about the PRE-POST experimental protocol can be found in (Bari et al., 2021). Briefly, we enrolled 19 patients scheduled for coronary artery bypass grafting (age: 64±8 yrs, all males). Subjects received pre-anesthesia with an intramuscular dose of atropine (0.5 mg) and fentanyl (100 μg). General intravenous anesthesia was then induced with a propofol bolus of 1.5 $mg \cdot kg^{-1}$ and maintained with a dose of 3 $mg \cdot kg^{-1} \cdot h^{-1}$ of propofol and a rate from 0.05 to 0.5 $\mu g \cdot kg^{-1} \cdot min^{-1}$ of remifentanil with a mean rate of 0.32 $\mu g \cdot kg^{-1} \cdot min^{-1}$. We acquired ECG from lead II and AP, derived invasively from the radial artery, and CBFV from the left middle cerebral artery, as obtained from a transcranial Doppler device (Multi-Dop X, DWL, San Juan Capistrano, CA, USA). Signals were acquired with a sampling rate of 1000 Hz for 6 minutes in each condition. Acquisitions took place in PRE and POST sessions. POST occurred after the intubation of the trachea but before opening the chest. POST session just followed the PRE one. POST session started when the target plasma concentration of propofol was expected to be around 3 $\mu g \cdot kg^{-1}$ based on the pharmacokinetic properties of the drug. Patients spontaneously breathed during PRE and were mechanically ventilated at a rate from 12 to 16 $breaths \cdot min^{-1}$ during POST.

3.4 Series extraction and data analysis

In both protocols, heart period (HP) was extracted as the time distance between consecutive R-wave peaks on the ECG. After identifying the R-wave the position of the R-wave peak was located via parabolic interpolation. MAP and MCBFV series were extracted by integrating the AP and CBFV signals respectively between two diastolic points and by normalizing the result by dividing it by the inter-diastolic interval (Bari et al., 2016). The ith value of MAP and MCBFV was computed over the same HP. Series were manually checked for missing beats and misdetections. The effect of ectopic beats was minimized via linear interpolation based on values associated to sinus beats. The fraction of corrections did not overcome 5% of the total length of the series. Stationary synchronous series of 250 beats were randomly chosen from each subject in each group in each experimental condition in both PRE-POST and REST-HUT protocols. Cardiovascular and cerebrovascular controls were characterized in time domain assessing mean and variance of each series, labeled respectively as μ_{HP}, μ_{MAP}, μ_{MCBFV}, σ^2_{HP}, σ^2_{MAP} and σ^2_{MCBFV} and expressed in ms, mmHg, $cm \cdot s^{-1}$, ms^2, $mmHg^2$ and $cm^2 \cdot s^{-2}$. Series were then linearly detrended before assessing variance and spectral indexes. The HP, MAP and MCBFV beat-to-beat variability were modeled via an autoregressive model, describing the series as a linear combination of past samples weighted by constant coefficients plus a zero mean white noise (Task Force, 1996). The order of the autoregressive model was optimized via Akaike's figure of merit in the range from 8 to 14 (Task Force, 1996). The power spectral density was factorized in components and classified according to their central frequency (Baselli et al., 1997). According to the definitions given in (Task Force, 1996), a component of HP series was labeled as low frequency (LF) if its central frequency ranged between 0.04 and 0.15 Hz and as high frequency (HF) if its central frequency dropped between 0.15 and 0.5 Hz. According to the definition given in (Claassen et al., 2016) a component of MAP and MCBFV series was labeled as very LF (VLF) if its central frequency dropped between 0.02 and 0.07 Hz, as LF if it was comprised between 0.07 and 0.15 Hz and as HF if it dropped between 0.15 and 0.5 Hz. The superior cut-off of the LF band and inferior cut-off of the HF band was reduced to 0.15 Hz from the one suggested in (Claassen et al., 2016), namely 0.2 Hz, to account for the possible presence of spontaneous, or paced, breathing rates below 0.2 Hz (Vaini et al., 2019). A parametric cross-spectral method, exploiting a bivariate autoregressive model (Porta et al., 2000), was used to describe the coupling between MAP and MCBFV. The order of the bivariate model was fixed to 10 (Porta et al., 2000). Squared coherence K^2 was calculated as the ratio of the square modulus of the cross-spectrum between MAP and MCBFV to the product of MAP and MCBFV power spectral densities (Vaini et al., 2019). K^2 values were computed as the average of the K^2 in VLF, LF and HF band (Bari et al., 2019), using the same limits defined for univariate analysis of MAP and MCBFV variabilities (Claassen et al., 2016). K^2 indexes were labeled as K^2_{VLF}, K^2_{LF} and K^2_{HF}.

3.5 Statistical analysis

A paired t-test, or a Wilcoxon signed rank test when appropriate, was applied to check the effect of the intervention (i.e. orthostatic stressor or general anesthesia) over time and frequency domain indexes calculated in the REST-HUT and PRE-POST protocols respectively. A two-way repeated measures analysis of variance (one factor repetition, Holm-Sidak test for multiple comparisons) was applied to NMSPE and ρ to check the significance of the difference between experimental condition (i.e. REST versus HUT and PRE versus POST) within the type of the series (i.e. original or surrogate series) and to test the significance of the difference between types of series given the experimental condition. The same statistical test was applied to optimal ARI values to assess the significance of the difference between experimental conditions (i.e. REST versus HUT and PRE versus POST) within the same metric (i.e. NMSPE or ρ) and to test the significance of the difference between metrics given the experimental condition. The χ^2 test was applied to the proportions of subjects with ARI>4 to assess the impact of the challenge (i.e. HUT or POST) within the same metric (i.e. NMSPE or ρ) and the impact of the figure of merit within an assigned experimental condition. The level of statistical significance of the χ^2 test was lowered according to the number of comparisons (i.e. 4) to account for the multiple comparison issue. Continuous variables are reported as mean ± standard deviation. Statistical analysis was performed with a commercial statistical software (Sigmaplot v.14.0, Systat Software, San Jose, CA, USA). The level of statistical significance of all the tests was set to 0.05.

4. Results

4.1. Time and frequency domain results

Table 1 shows univariate time and frequency domain parameters derived from HP, MAP and MCBFV variability series in the REST-HUT protocol. HUT induced a shortening of μ_{HP} and a reduction of HFa_{HP}. σ^2_{HP} and LFa_{HP} did not vary with the postural challenge. HUT increased LFa_{MAP}. Conversely, μ_{MAP}, σ^2_{MAP}, $VLFa_{MAP}$ and HFa_{MAP} were not affected by the orthostatic stressor. μ_{MCBFV} was reduced during HUT, while LFa_{MCBFV} and HFa_{MCBFV} were significantly increased. σ^2_{MCBFV} and $VLFa_{MCBFV}$ did not vary with the postural stimulus. Table 2 summarizes K^2 in VLF, LF and HF bands computed between MAP and MCBFV variability series in the REST-HUT protocol. Regardless of the frequency band, K^2 increased during HUT.

Univariate time and frequency domain parameters derived from HP, MAP and MCBFV time series in the PRE-POST protocol were reported in Tab.3. μ_{HP} increased during POST, while σ^2_{HP}, LFa_{HP} and HFa_{HP} decreased. μ_{MAP}, σ^2_{MAP}, $VLFa_{MAP}$ and LFa_{MAP} were significantly reduced during

POST as well as σ^2_{MCBFV} and $VLFa_{MCBFV}$. HFa_{MAP}, μ_{MCBFV}, LFa_{MCBFV} and HFa_{MCBFV} did not vary after the induction of propofol-based general anesthesia. Table 4 summarizes K^2 in VLF, LF and HF bands computed between MAP and MCBFV variability series in the PRE-POST protocol. Regardless of the frequency band, K^2 declined toward 0 during POST.

4.2. Results of metrics for ARI estimation

The grouped error bar graphs in Fig.1 show NMSPE assessed according to TDM (Fig.1a), nonPM based on SR (Fig.1b), PM based on IR (Fig.1c), and PM based on SR (Fig.1d) assessed over original (black bars) and surrogate (white bars) pairs as a function of the experimental condition (i.e. REST and HUT). Regardless of the experimental condition and method exploited to estimate ARI (i.e. TDM, nonPM based on SR, PM based on IR and PM based on SR), NMSPE was higher over the surrogate unmatched pairs than over the original matched ones (Figs.1a,b,c,d). A significant effect of the orthostatic challenge was visible in the analysis of original couples exclusively when $NMSPE_{TDM}$ was considered (Fig.1a) and it was never present in surrogates (Figs.1a,b,c,d).

Figure 2 has the same layout as Fig.1 but the different panels show ρ computed via TDM (Fig.2a), nonPM based on SR (Fig.2b), PM based on IR (Fig.2c), and PM based on SR (Fig.2d). ρ was lower over the surrogate series than over the original ones and this conclusion held regardless of the experimental condition and method exploited to estimate ARI (Figs.2a,b,c,d). In general, ρ was higher during HUT than at REST in original pairs but this result was significant solely when ρ_{TDM} and $\rho_{PM,IR}$ were considered (Figs.2a,c). No significant REST-HUT changes were observed over surrogates (Figs.2a,b,c,d).

Figure 3 has the same structure as Fig.1 but it monitors NMSPE in the PRE-POST protocol. The ability of NMSPE in distinguishing surrogate and original pairs and in detecting the impact of general anesthesia was limited. Original and surrogate couples could be evidently differentiated in both PRE and POST solely by the TDM (Fig.3a). Regardless of the type of series and method exploited to estimate ARI, the influence of propofol-based general anesthesia was not detectable (Figs.3a,b,c,d).

Figure 4 has the same layout as Fig.1 but it monitors ρ in the PRE-POST protocol. Regardless of the method for ARI estimation (Figs.4a,b,c,d), ρ was higher over the original than over surrogate data in both PRE and POST sessions. Over the original couples POST decreased significantly ρ compared to PRE solely when $\rho_{PM,IR}$ and $\rho_{PM,SR}$ were considered (Figs.4c,d). The effect of general anesthesia was not visible over surrogates (Figs.4a,b,c,d).

4.3. Results of ARI

The grouped error bar graphs of Fig.5 show the optimal ARI assessed according to TDM (Fig.5a), nonPM based on SR (Fig.5b), PM based on IR (Fig.5c), and PM based on SR (Fig.5d). The estimation of the optimal ARI was carried out according to the two different metrics, namely NMSPE (black bars) and ρ (white bars), as a function of the experimental condition in the REST-HUT protocol. ARI did not vary with type of metric and experimental condition and this conclusion held regardless of the method for ARI estimation (Figs.5,a,b,c,d).

Figure 6 has the same structure as Fig.5 but it shows the optimal ARI assessed in the PRE-POST protocol. Similarly to Fig.5, metric, experimental condition or method of ARI computation did not affect the optimal ARI (Figs.6,a,b,c,d).

The grouped bar graphs of Fig.7 show the percentage of subjects with ARI larger than 4, namely the percentage of subjects with a working CA, according to TDM (Fig.7a), nonPM based on SR (Fig.7b), PM based on IR (Fig.7c), and PM based on SR (Fig.7d). The assessment of the percentage was carried out according to the two different metrics, namely NMSPE (black bars) and ρ (white bars), as a function of the experimental condition in the REST-HUT protocol. The percentage of subjects with ARI larger than 4 did not differ across metrics, experimental conditions, or techniques for ARI computation (Figs.7,a,b,c,d).

Figure 8 has the same structure as Fig.7 but it shows the percentage of subjects with ARI larger than 4 in the PRE-POST protocol. Similarly to Fig.7, metric, experimental condition or method for ARI computation had no influence on the percentage of subjects with ARI larger than 4 (Figs.8,a,b,c,d).

5. Discussion

The main findings of the work can be summarized as follows: i) both NMSPE and ρ metrics were appropriate for ARI evaluation in the REST-HUT protocol; ii) ρ metric was preferable to NMSPE for its better ability to separate original from surrogate pairs in the PRE-POST protocol; iii) the ARIs estimated via NMSPE and ρ metrics were similar; iv) CA was not affected by either postural challenge or propofol-based general anesthesia and this conclusion held regardless of the technique for ARI estimation and metric utilized for the comparison between measured and predicted MCBFV series.

5.1. NMSPE and ρ have different abilities in separating original and surrogate couples

We tested two different metrics for the assessment of ARI in connection with methods for the evaluation of CA based on spontaneous MAP and MCBFV variabilities and Tiecks' model as reviewed in (Gelpi et al., 2021). In the REST-HUT protocol, both NMSPE and ρ metrics appeared to

be appropriate for ARI evaluation given that they were able to distinguish between original and surrogate couples and this conclusion held regardless of the technique utilized for ARI estimation. In the PRE-POST protocol, ρ metric was preferable to NMSPE given that NMPSE was much more ineffective in distinguishing original from surrogate pairs (e.g. in the case of utilization of nonPM and PM techniques).

The possible reason of the different conclusions about the ability of NMSPE and ρ in the REST-HUT and PRE-POST protocols is the diverse degree of association between MAP and MCBFV in the two experimental protocols. Indeed, while K^2 increased during HUT compared to REST in the REST-HUT protocol (Tab.2), K^2 declined toward 0 in POST compared to PRE in the PRE-POST protocol (Tab.4). These trends of K^2 confirmed our previous studies (Bari et al., 2017; Bari et al., 2021). This diverse conclusion in the two experimental protocols made clearer peculiar differences of metrics utilized for testing similarities between measured, or data-driven, MCBFV series and the version predicted by Tiecks' model. Indeed, a method, such as TDM, that does not strictly require a sufficient level of agreement between original MAP and MCBFV because it does not exploit these two series simultaneously but uses only the original MAP to predict MCBFV (Panerai et al., 2003; Mahdi et al., 2017), is able to distinguish original from surrogate pairs even in PRE-POST protocol regardless of the metric utilized to compare measured and predicted MCBFV series. Conversely, methods that require a sufficient degree of association between measured MAP and MCBFV to be reliable, such as nonPM and PM, because they are based on the identification of nonparametric and parametric MAP-MCBFV relationship respectively (Panerai et al., 1998; Panerai et al., 1999; Simpson et al., 2001), are able to separate original from surrogate pairs exclusively using ρ. As a matter of fact, ρ is less sensible to the magnitude of the absolute changes between measured and predicted MCBFV variability than NMSPE and this robustness might have limited the consequence of the poor reliability of MCBFV-MAP relationship estimated from weakly associated original MAP and MCBFV series.

Thus, we conclude that the use of ρ is recommended in presence of weakly interacting MAP and MCBFV variability series especially whether methods necessitating a significant level of association between MAP and MCBFV series, such as nonPM and PM, are applied.

5.2. NMSPE and ρ did not lead to different ARI estimates in both REST-HUT and PRE-POST protocols

It is worth noting that, when ARI values derived from NMSPE and ρ were compared in both REST-HUT and PRE-POST protocols, no significant differences were detected. This conclusion held regardless of the experimental condition and technique for ARI estimation. The main consequence is

the agreement of NMSPE and ρ about the irrelevance of the challenge on CA in the two protocols. In a previous study we compared directly the values of ARIs derived from different methods (i.e. TDM, nonPM and PM) using the NMSPE metric and we found that subtle differences might exist even though these differences might not imply diverse final conclusions (Gelpi et al., 2021). In particular, we observed that TDM might provide ARIs smaller than those derived from nonPM and PM (Gelpi et al., 2021). Even though in the present study ARIs derived from the different methods were not directly compared, we can confirm the tendency of observing smaller ARI values with TDM resulting in the smaller percentage of subjects with ARI larger than 4 in PRE session compared to nonPM and PM techniques. Remarkably, trends in the ARI values could not be attributed to the metric utilized to compare measured, or data-driven, and predicted MCBFV series given that no differences between ARIs derived from NMSPE and ρ were detected.

5.3. CA is not influenced by either postural challenge or propofol-based general anesthesia

REST-HUT and PRE-POST protocols induced an important modification of the autonomic control and baroreflex function. During HUT we observed a sympathetic activation (Cooke et al., 1999; Furlan et al., 2000; Marchi et al., 2016), a vagal withdrawal (Montano et al., 1994; Cooke et al., 1999; Porta et al., 2007b) and a reduced baroreflex sensitivity (Cooke et al., 1999; Porta, et al., 2016; De Maria et al., 2019). During propofol-based general anesthesia autonomic depression is mainly the result of reduced sympathetic control leading to vasodilatation, reduced ventricular contractility and reduction of peripheral resistance (Ebert et al., 1992; Sellgren et al., 1994; Boer et al., 1990) and it was accompanied by a dampened baroreflex sensitivity (Keyl et al., 2000; Sato et al., 2005; Porta et al., 2013; Bari et al., 2019). Given that sympathetic control is a determinant of the CA (Zhang et al., 2002; Hamner et al., 2010), it might be expected that CA was altered in both REST-HUT and PRE-POST protocols. Conversely, regardless of the method and metric used to assess ARI, ARI was not modified by gravitational stimulus and propofol-based general anesthesia. As a consequence, we can conclude that CA remained unmodified with a postural challenge in healthy subjects or the induction of propofol-based general anesthesia in patients scheduled for coronary artery bypass grafting. This conclusion agrees with several studies carried out during HUT (Carey et al., 2001; Schondorf et al., 2001; Claydon and Hainsworth, 2003; Castro et al., 2017; Bari et al., 2017; Gelpi et al., 2021) and in POST (Strebel et al., 1995; Engelhard et al., 2001; Ogawa et al., 2010) and it is corroborated by the use of different strategies and metrics for the ARI assessment. This conclusion appears to be particularly robust because it is supported by all the techniques of ARI estimation and by both the metrics for testing the similarity between measured and predicted MCBFV variability. In particular, it held when the technique and metric that appears to be more robust in

presence of low level of association between original MAP and MCBFV variabilities was exploited, namely the TDM based on computation of ρ. The limited influence of orthostatic challenge and propofol-based general anesthesia was supported by the variability markers as well (Claassen et al., 2016). Indeed, in the REST-HUT protocol of σ^2_{MAP} and σ^2_{MCBFV} did not vary during HUT compared to REST and the increased of LFa_{MCBFV} was explained by the increase of LFa_{MAP}, thus leaving unaltered the MCBFV-MAP transfer function gain (Zhang et al., 1998). In the PRE-POST protocol the invariance of CA was confirmed by the simultaneous decrease of both σ^2_{MAP} and σ^2_{MCBFV} during POST compared to PRE and by the smallness of MCBFV fluctuations in all frequency bands during POST.

6. Conclusions

This work tested two figures of merit (i.e. NMSPE and ρ) for the assessment of the level of agreement between measured, or data-driven, MCBFV variability and the version predicted by the use of Tiecks' differential equations. This evaluation was carried out in experimental protocols designed to have a profound impact on autonomic control, namely an orthostatic challenge and propofol-based general anesthesia. We recommend the use of ρ in practical contexts featuring a low degree of association between MAP and MCBFV variability that might reduce the reliability of methods for ARI assessment (e.g. nonPM and PM) because this norm might reduce the detrimental effect of important departures between measured and predicted MCBFV dynamics. Despite the differences between the two metrics, similar conclusions about the negligible impact of an orthostatic challenge and propofol-based general anesthesia on CA are drawn. Conclusions seem to suggest a limited impact of the sympathetic control on CA. Even though results indicate that metrics utilized for comparing measured and predicted MCBFV might not influence final conclusions, the observed difference between NMSPE and ρ suggests caution when comparing studies using different metrics, especially when the level of association between spontaneous fluctuations of MAP and MCBFV is weak, such as in impaired CA.

Funding. This work was partially supported to Ricerca Corrente of the Italian Ministry of Health to IRCCS Policlinico San Donato.

Contributions. Vlasta Bari: Conceptualization, Methodology, Software, Formal Analysis, Visualization, Data Curation, Investigation, Resources, Writing - Original draft preparation, Writing - Review & Editing. Lorenzo Barbarossa: Software, Formal Analysis, Data Curation, Writing - Review & Editing. Francesca Gelpi: Methodology, Software, Data Curation, Writing - Review & Editing. Beatrice Cairo: Data Curation, Writing - Review & Editing. Beatrice De Maria: Data Curation, Writing - Review & Editing. Davide Tonon: Investigation, Data Curation, Writing - Review & Editing. Gianluca Rossato: Investigation, Data Curation, Resources, Writing - Review & Editing.

476 Luca Faes: Writing - Review & Editing. Marco Ranucci: Resources, Writing - Review & Editing.
477 Riccardo Barbieri: Conceptualization, Methodology, Writing - Review & Editing, Supervision.
478 Alberto Porta: Conceptualization, Methodology, Software, Visualization, Resources, Writing -
479 Original draft preparation, Writing - Review & Editing, Supervision.
480

481 **Conflicts of Interest.** The authors declare no conflict of interest.
482

483

References

Task Force of the European Society of Cardiology and the North American Society of Pacing and Electrophysiology, 1996. Heart rate variability. Standards of measurement, physiological interpretation, and clinical use. Eur. Heart J. 17, 354–381.

Aaslid, R., Lindegaard, K.F., Sorteberg, W., et al., 1989. Cerebral autoregulation dynamics in humans. Stroke 20, 45–52.

Aaslid, R., Markwalder, T.M., Nornes, H., 1982. Noninvasive transcranial Doppler ultrasound recording of flow velocity in basal cerebral arteries. J. Neurosurg. 57, 769–774.

Angarita-Jaimes, N., Kouchakpour, H., Liu, J., et al., 2014. Optimising the assessment of cerebral autoregulation from black box models. Med. Eng. Phys. 36, 607–612.

Bari, V., De Maria, B., Mazzucco, et al., 2017. Cerebrovascular and cardiovascular variability interactions investigated through conditional joint transfer entropy in subjects prone to postural syncope. Physiol. Meas. 38, 976–991.

Bari, V., Fantinato, A., Vaini, E., et al., 2021. Impact of propofol general anesthesia on cardiovascular and cerebrovascular closed loop variability interactions. Biomed. Signal Process. Control 68, 102735.

Bari, V., Marchi, A., De Maria, B., et al., 2016 Nonlinear effects of respiration on the crosstalk between cardiovascular and cerebrovascular control systems. Phil. Trans. R. Soc. A, 374, 20150179.

Bari, V., Vaini, E., Pistuddi, V., et al., 2019. Comparison of causal and non-causal strategies for the assessment of baroreflex sensitivity in predicting acute kidney dysfunction after coronary artery bypass grafting. Front. Physiol. 10, 1319.

Baselli, G., Porta, A., Rimoldi, O., et al., 1997. Spectral decomposition in multichannel recordings based on multi-variate parametric identification. IEEE Trans. Biomed. Eng. 44, 1092–1101.

Boer, F., Ros, P., Bovill, J.G., et al., 1990. Effect of propofol on peripheral vascular resistance during cardiopulmonary bypass. Br. J. Anaesth. 65, 184–189.

Carey, B.J., Manktelow, B.N., Panerai, R.B., et al., 2001. Cerebral autoregulatory responses to head-up tilt in normal subjects and patients with recurrent vasovagal syncope. Circulation 104, 898–902.

Castro, P.M., Santos, R., Freitas, et al., 2014. Autonomic dysfunction affects dynamic cerebral autoregulation during Valsalva maneuver: comparison between healthy and autonomic dysfunction subjects. J. Appl. Physiol. 117, 205–213.

Castro, P., Freitas, J., Santos, R., et al., 2017. Indexes of cerebral autoregulation do not reflect impairment in syncope: insights from head-up tilt test of vasovagal and autonomic failure subjects. Eur. J. Appl. Physiol. 117, 1817–1831.

Claassen, J.A., Meel-van den Abeelen, A.S., Simpson, D.M., et al., on behalf of the International Cerebral Autoregulation Research Network (CARNet). 2016. Transfer function analysis of dynamic cerebral autoregulation: A white paper from the International Cerebral Autoregulation Research Network. J. Cereb. Blood Flow Metab. 36, 665–680.

Claydon, V.E., Hainsworth, R., 2003. Cerebral autoregulation during orthostatic stress in healthy controls and in patients with posturally related syncope. Clin. Auton. Res. 13, 321–329.

Cooke, W.H., Hoag, J.B., Crossman, A.A., et al., 1999. Human responses to upright tilt: a window on central autonomic integration. J. Physiol. 517, 617–628.

Czosnyka, M., Smielewski, P., Lavinio, A., et al., 2008. An assessment of dynamic autoregulation from spontaneous fluctuations of cerebral blood flow velocity: a comparison of two models, index of autoregulation and mean flow index. Anesth. Analg. 106, 234–239.

Dawson, S.L., Blake, M.J., Panerai, R.B., et al., 2000. Dynamic but not static cerebral autoregulation is impaired in acute ischaemic stroke. Cerebrovasc. Dis. 10, 126–132.

De Maria, B., Bari, V., Cairo, B., et al., 2019. Characterization of the asymmetry of the cardiac and sympathetic arms of the baroreflex from spontaneous variability during incremental head-up tilt. Front. Physiol. 10, 342.

Dineen, N.E., Brodie, F.G., Robinson, T.G., et al., 2010. Continuous estimates of dynamic cerebral autoregulation during transient hypocapnia and hypercapnia. J. Appl. Physiol. 108, 604–613.

Ebert, T.J., Muzi, M., Berens, R., et al., 1992. Sympathetic responses to induction of anesthesia in humans with propofol or etomidate. Anesthesiology 76, 725–733.

Engelhard, K., Werner, C., Möllenberg, O., et al., 2001. Effects of remifentanil/propofol in comparison with isoflurane on dynamic cerebrovascular autoregulation in humans Acta Anaesthesiol. Scand. 45, 971-976.

Faes, L., Porta, A., Rossato, G., et al., 2013. Investigating the mechanisms of cardiovascular and cerebrovascular regulation in orthostatic syncope through an information decomposition strategy. Auton. Neurosci.: Basic Clin. 178, 76–82.

Furlan, R., Porta, A., Costa, F., et al., 2000. Oscillatory patterns in sympathetic neural discharge and cardiovascular variables during orthostatic stimulus. Circulation 101, 886–892.

Gelpi, F., Bari, V., Cairo, et al., 2021. Dynamic cerebrovascular autoregulation in patients prone to postural syncope: comparison of techniques assessing the autoregulation index from spontaneous variability series. Auton. Neurosci.: Basic Clin. (submitted).

Hamner, J.W., Tan, C.O., Lee, K., et al., 2010. Sympathetic control of the cerebral vasculature in humans. Stroke 41, 102–109.

Keyl, C., Schneider, A., Dambacher, M., et al., 2000. Dynamic cardiocirculatory control during propofol anesthesia in mechanically ventilated patients. Anesth. Analg. 91, 1188–1195.

Lassen, N.A., 1959. Cerebral blood flow and oxygen consumption in man. Physiol. Rev. 39, 183–238.

Lee, Y.K., Rothwell, P.M., Payne, S.J., et al., 2020. Reliability, reproducibility and validity of dynamic cerebral autoregulation in a large cohort with transient ischaemic attack or minor stroke. Physiol. Meas. 41, 095002.

Mahdi, A., Nikolic, D., Birch, A.A., et al., 2017. Increased blood pressure variability upon standing up improves reproducibility of cerebral autoregulation indices. Med. Eng. Phys. 47, 151–158.

Marchi, A., Bari, V., De Maria, B., et al., 2016. Calibrated variability of muscle sympathetic nerve activity during graded head-up tilt in humans and its link with noradrenaline data and cardiovascular rhythms. Am. J. Physiol. 310, R1134–R1143.

Montano, N., Gnecchi-Ruscone, T., Porta, A., et al., 1994. Power spectrum analysis of heart rate variability to assess changes in sympatho-vagal balance during graded orthostatic tilt. Circulation 90, 1826–1831.

Newell, D.W., Aaslid, R., Lam, A., et al., 1994. Comparison of flow and velocity during dynamic autoregulation testing in humans. Stroke 25, 793–797.

Ogawa, Y., Iwasaki, K., Aoki, K., et al., 2010. The different effects of midazolam and propofol sedation on dynamic cerebral autoregulation. Anesth. Analg. 111, 1279–1284.

Panerai, R.B., Dawson, S.L., Eames, P.J., et al., 2001. Cerebral blood flow velocity response to induced and spontaneous sudden changes in arterial blood pressure. Am. J. Physiol. 280, H2162–H2174.

Panerai, R.B., Dawson, S.L., Potter, J.F., 1999. Linear and nonlinear analysis of human dynamic cerebral autoregulation. Am. J. Physiol. 277, H1089–H1099.

Panerai, R.B., Eames, P.J., Potter, J.F., 2003. Variability of time-domain indices of dynamic cerebral autoregulation. Physiol. Meas. 24, 367–381.

Panerai, R.B., Haunton, V.J., Minhas, J.S., et al., 2018. Inter-subject analysis of transfer function coherence in studies of dynamic cerebral autoregulation. Physiol. Meas. 39, 125006.

Panerai, R.B., White, R.P., Markus, H.S., et al., 1998. Grading of cerebral dynamic autoregulation from spontaneous fluctuations in arterial blood pressure. Stroke 29, 2341–2346.

Paulson, O.B., Strandgaard, S., Edvinsson, L., 1990. Cerebral autoregulation. Cerebrovasc. Brain Metab. Rev. 2, 161–192.

Penzel, T., Porta, A., Stefanovska, A., et al., 2017. Recent advances in physiological oscillations. Physiol. Meas. 38, E1-E7.

Porta, A., Bari, V., Bassani, T., et al., 2013. Model-based causal closed-loop approach to the estimate of baroreflex sensitivity during propofol anesthesia in patients undergoing coronary artery bypass graft. J. Appl. Physiol. 115, 1032–1042.

Porta, A., Baselli, G., Rimoldi, O., et al., 2000. Assessing baroreflex gain from spontaneous variability in conscious dogs: role of causality and respiration. Am. J. Physiol. 279, H2558–H2567.

Porta, A., Guzzetti, S., Furlan, R., et al., 2007a. Complexity and nonlinearity in short-term heart period variability: comparison of methods based on local nonlinear prediction. IEEE Trans. Biomed. Eng. 54, 94–106.

Porta, A., Takahashi, A.C.M., Catai, A.M., 2016. Cardiovascular coupling during graded postural challenge: comparison between linear tools and joint symbolic analysis. Braz. J. Phys. Ther. 20, 461–470.

Porta, A., Tobaldini, E., Guzzetti, S., et al., 2007b. Assessment of cardiac autonomic modulation during graded head-up tilt by symbolic analysis of heart rate variability. Am. J. Physiol. 293, H702–H708.

Sato, M., Tanaka, M., Umehara, S., et al., 2005. Baroreflex control of heart rate during and after propofol infusion in humans. Br. J. Anaesth. 94, 577–581.

Schondorf, R., Stein, R., Roberts, R., et al., 2001. Dynamic cerebral autoregulation is preserved in neurally mediated syncope. J. Appl. Physiol. 91, 2493–2502.

Sellgren, J., Ejnell, H., Elam, M., et al., 1994. Sympathetic muscle nerve activity, peripheral blood flows, and baroreceptor reflexes in humans during propofol anesthesia and surgery. Anesthesiology 80, 534–544.

Simpson, D.M., Panerai, R.B., Evans, D.H., et al., 2001. A parametric approach to measuring cerebral blood flow autoregulation from spontaneous variations in blood pressure. Ann. Biomed. Eng. 29, 18–25.

Strandgaard, S., Paulson, O.B., 1984. Cerebral autoregulation. Stroke 15, 413–416.

Strebel, S., Lam, A.M., Matta, B., et al., 1995. Dynamic and static cerebral autoregulation during isoflurane, desflurane, and propofol anesthesia. Anesthesiology 83, 66–76.

610 Tiecks, F.P., Lam, A.M., Aaslid, R., et al., 1995. Comparison of static and dynamic cerebral
611 autoregulation measurements. Stroke 26, 1014–1019.

612 Vaini, E., Bari, V., Fantinato, A., et al., 2019. Causality analysis reveals the link between
613 cerebrovascular control and acute kidney dysfunction after coronary artery bypass grafting. Physiol.
614 Meas. 40, 064006.

615 Van Leeuwen, P., Geue, D., Lange, S., et al., 2003. Is there evidence of fetal-maternal heart rate
616 synchronization? BMC Physiol. 3, 2.

617 Zhang, R. Zuckerman, J.H. Iwasaki, K. et al., 2002. Autonomic neural control of dynamic cerebral
618 autoregulation in humans. Circulation 106, 1814–1820.

619 Zhang, R. Zuckerman, J.H. Giller, C.A. et al., 1998. Transfer function analysis of dynamic cerebral
620 autoregulation in humans. Am. J. Physiol. 274, H233–H241.

621

622

Figure captions

Fig.1. The grouped error bar graphs show NMSPE computed in correspondence of the optimal ARI through TDM (a), nonPM based on SR (b), PM based on IR (c) and PM based on SR (d) in the REST-HUT protocol. NMSPE is reported as a function of the experimental condition (i.e. REST and HUT) assessed over original (black bars) and surrogate (white bars) pairs of series. The symbol * indicates a significant difference between the original and surrogate pairs within the same experimental condition, while the symbol § indicates a significant difference between experimental conditions within the same type of analysis with $p<0.05$.

Fig.1. The grouped error bar graphs show ρ computed in correspondence of the optimal ARI through TDM (a), nonPM based on SR (b), PM based on IR (c) and PM based on SR (d) in the REST-HUT protocol. ρ is reported as a function of the experimental condition (i.e. REST and HUT) assessed over original (black bars) and surrogate (white bars) pairs of series. The symbol * indicates a significant difference between the original and surrogate pairs within the same experimental condition, while the symbol § indicates a significant difference between experimental conditions within the same type of analysis with $p<0.05$.

Fig.3. The grouped error bar graphs show NMSPE computed in correspondence of the optimal ARI through TDM (a), nonPM based on SR (b), PM based on IR (c) and PM based on SR (d) in the PRE-POST protocol. NMSPE is reported as a function of the experimental condition (i.e. PRE and POST) assessed over original (black bars) and surrogate (white bars) pairs of series. The symbol * indicates a significant difference between the original and surrogate pairs within the same experimental condition, while the symbol § indicates a significant difference between experimental conditions within the same type of analysis with $p<0.05$.

Fig.4. The grouped error bar graphs show ρ computed in correspondence of the optimal ARI through TDM (a), nonPM based on SR (b), PM based on IR (c) and PM based on SR (d) in the PRE-POST protocol. ρ was reported as a function of the experimental condition (i.e. PRE and POST) assessed over original (black bars) and surrogate (white bars) pairs of series. The symbol * indicates a significant difference between the original and surrogate pairs within the same experimental condition, while the symbol § indicates a significant difference between experimental conditions within the same type of analysis with $p<0.05$.

Fig.5. The grouped error bar graphs show the optimal ARI estimated via TDM (a), nonPM based on SR (b), PM based on IR (c) and PM based on SR (d) in the REST-HUT protocol. The optimal ARI is reported as a function of the experimental condition (i.e. REST and HUT) assessed over original (black bars) and surrogate (white bars) pairs. The symbol * indicates a significant difference between the original and surrogate couples within the same experimental condition with $p<0.05$.

Fig.6. The grouped error bar graphs show the optimal ARI estimated via TDM (a), nonPM based on SR (b), PM based on IR (c) and PM based on SR (d) in the PRE-POST protocol. The optimal ARI is reported as a function of the experimental condition (i.e. PRE and POST) assessed over original (black bars) and surrogate (white bars) pairs. The symbol * indicates a significant difference between the original and surrogate couples within the same experimental condition with $p<0.05$.

Fig.7. The grouped bar graphs show the percentage of the optimal ARI greater than 4 estimated via TDM (a), nonPM based on SR (b), PM based on IR (c) and PM based on SR (d) in the REST-HUT protocol. The percentage of the optimal ARI greater than 4 is reported as a function of the experimental condition (i.e. REST and HUT) assessed through the NMSPE (black bars) and ρ (white bars) metrics. The symbol * indicates a significant difference between the original and surrogate pairs within the same experimental condition with $p<0.05$.

Fig.8. The grouped bar graphs show the percentage of the optimal ARI greater than 4 estimated via TDM (a), nonPM based on SR (b), PM based on IR (c) and PM based on SR (d) in the PRE-POST

670 protocol. The percentage of the optimal ARI greater than 4 is reported as a function of the
671 experimental condition (i.e. PRE and POST) assessed through the NMSPE (black bars) and ρ (white
672 bars) metrics. The symbol * indicates a significant difference between the original and surrogate pairs
673 within the same experimental condition with $p<0.05$.

674

675

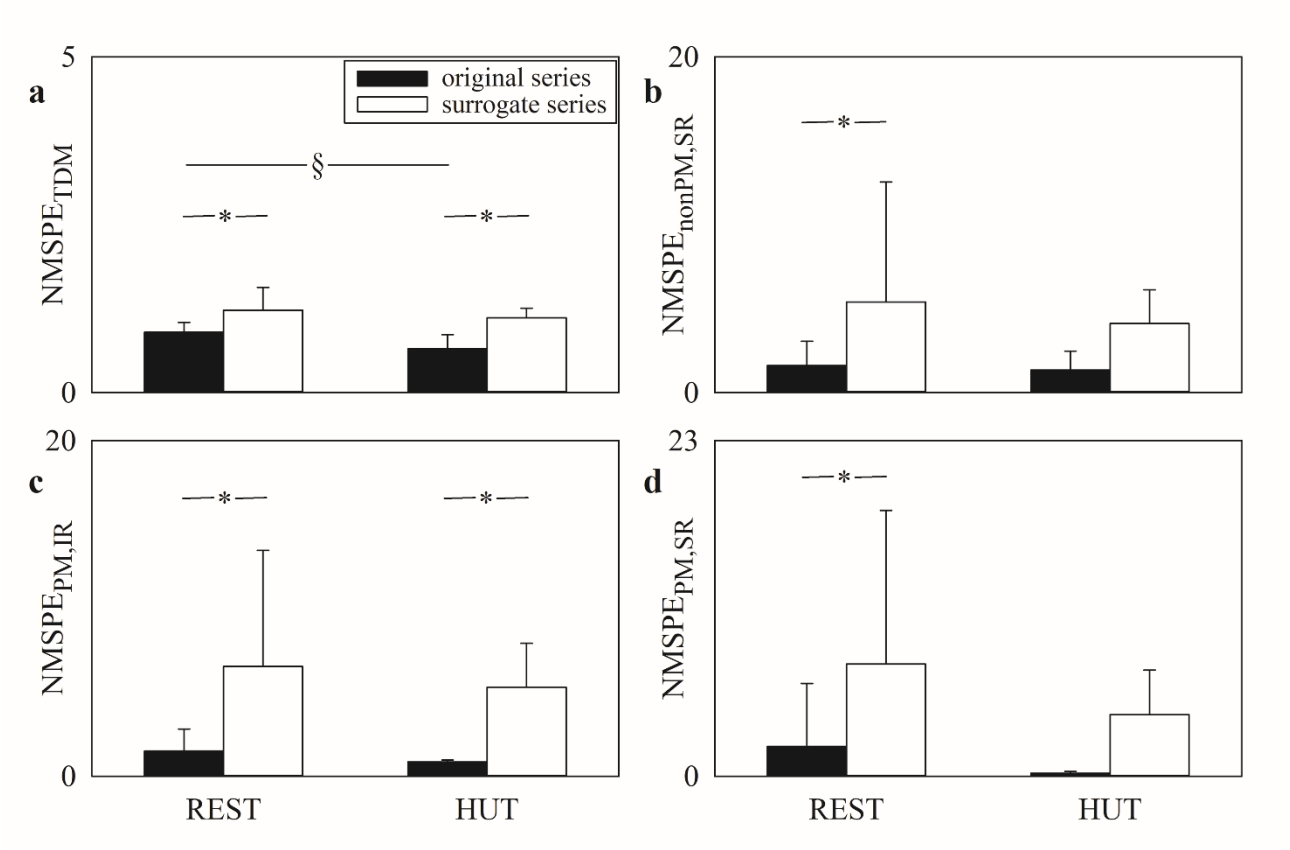

676

677 Fig. 1

678

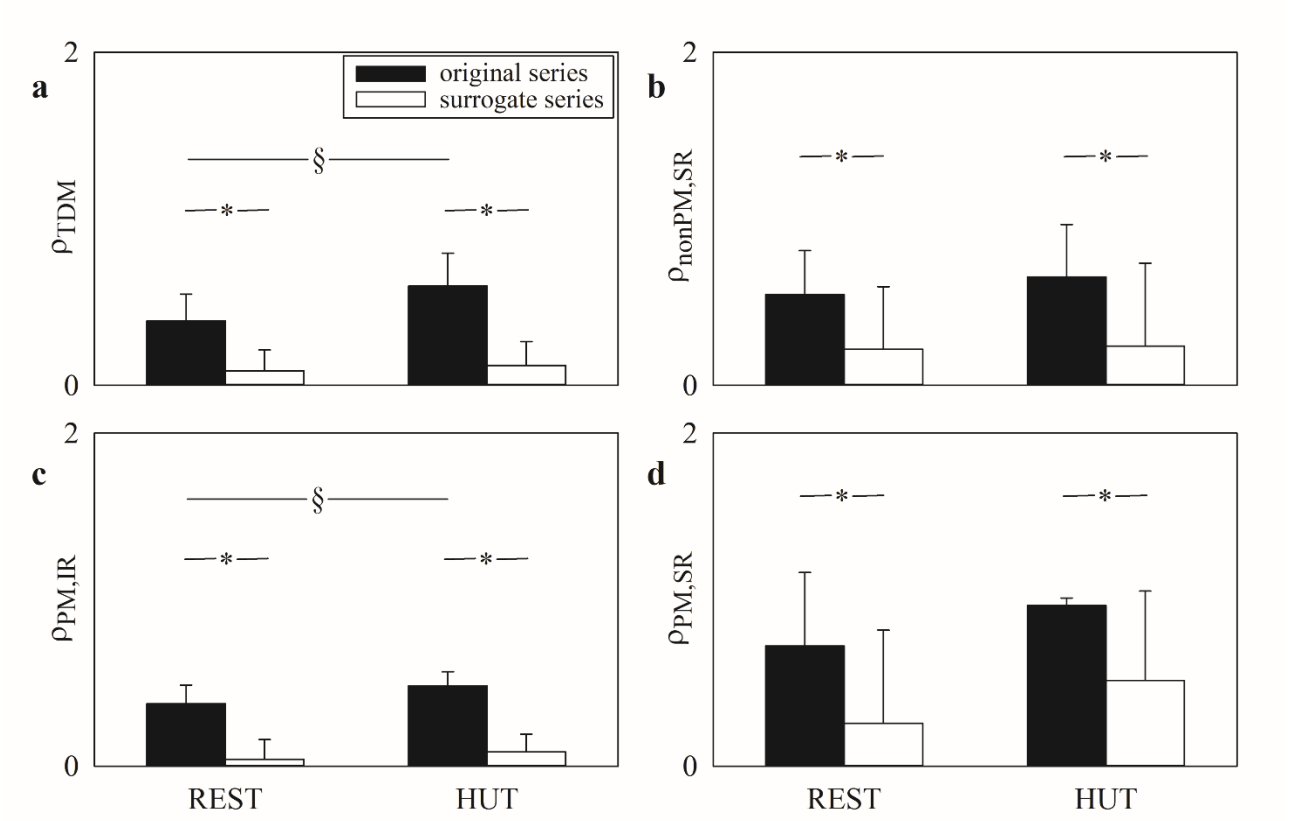
a
b
c
d
original series
surrogate series
ρTDM
ρnonPM,SR
ρPM,IR
ρPM,SR
2
0
§
*
REST
HUT

Fig. 2

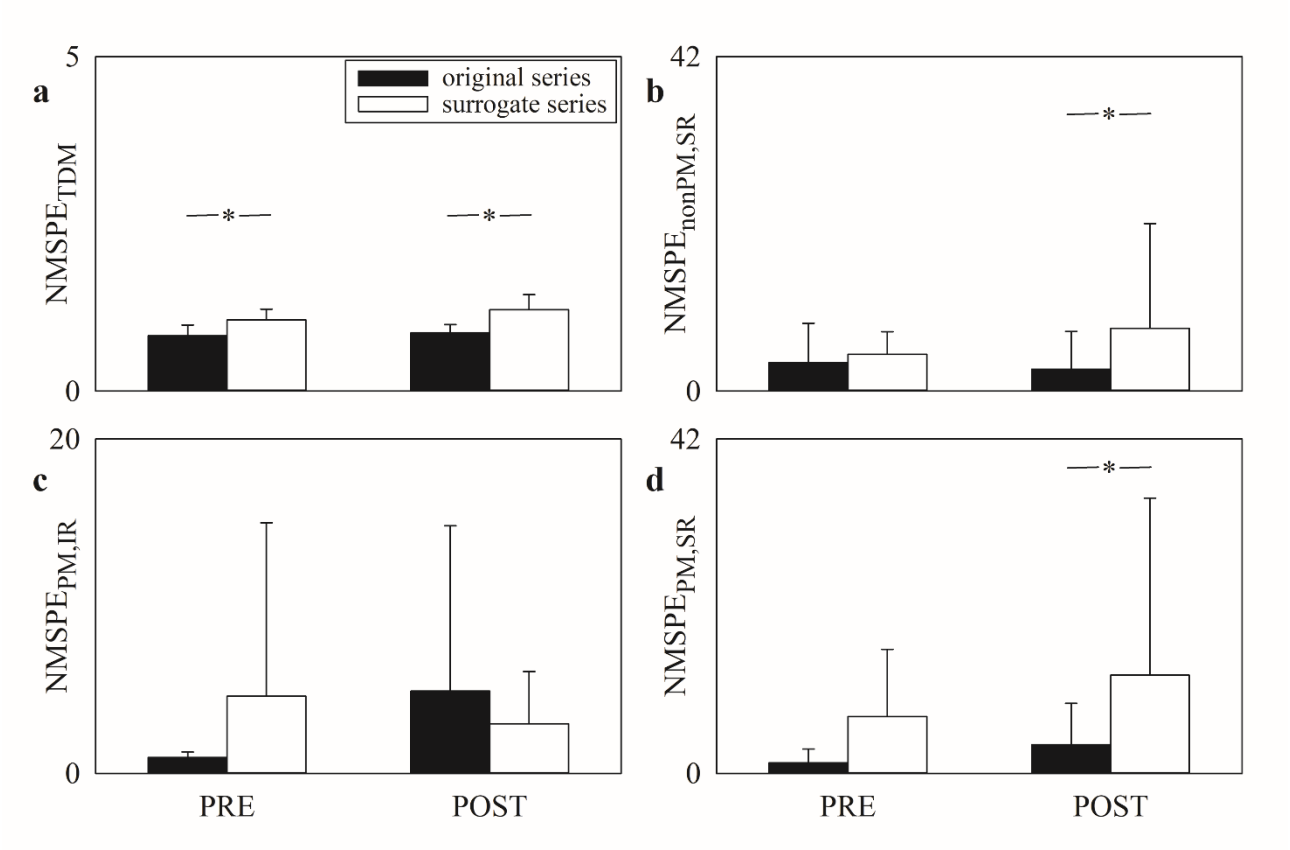
a
b
c
d
original series
surrogate series
NMSPE_TDM
NMSPE_nonPM,SR
NMSPE_PM,IR
NMSPE_PM,SR
5
0
42
0
20
0
42
0
*
PRE
POST

Fig. 3

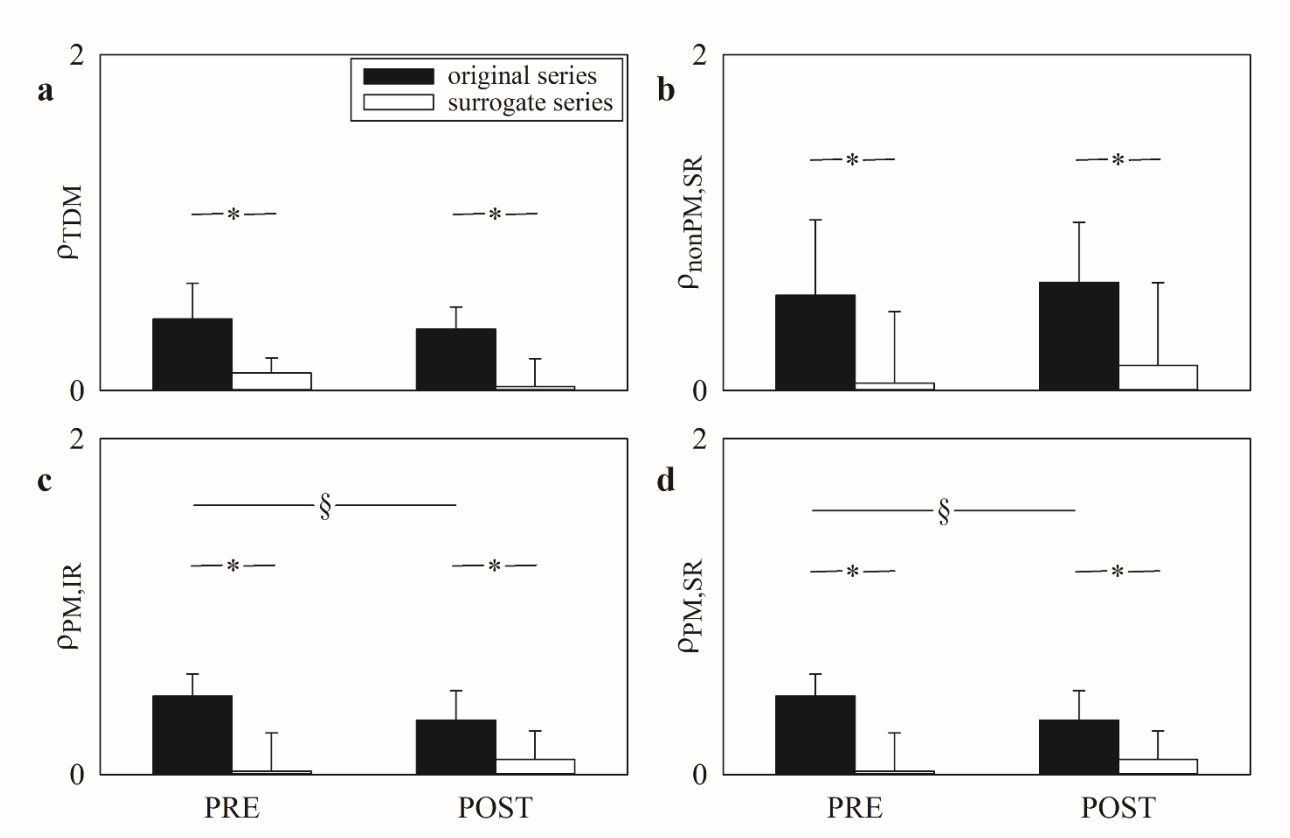
a
b
c
d
original series
surrogate series
ρTDM
ρnonPM,SR
ρPM,IR
ρPM,SR
2
0
*
§
PRE
POST

Fig. 4

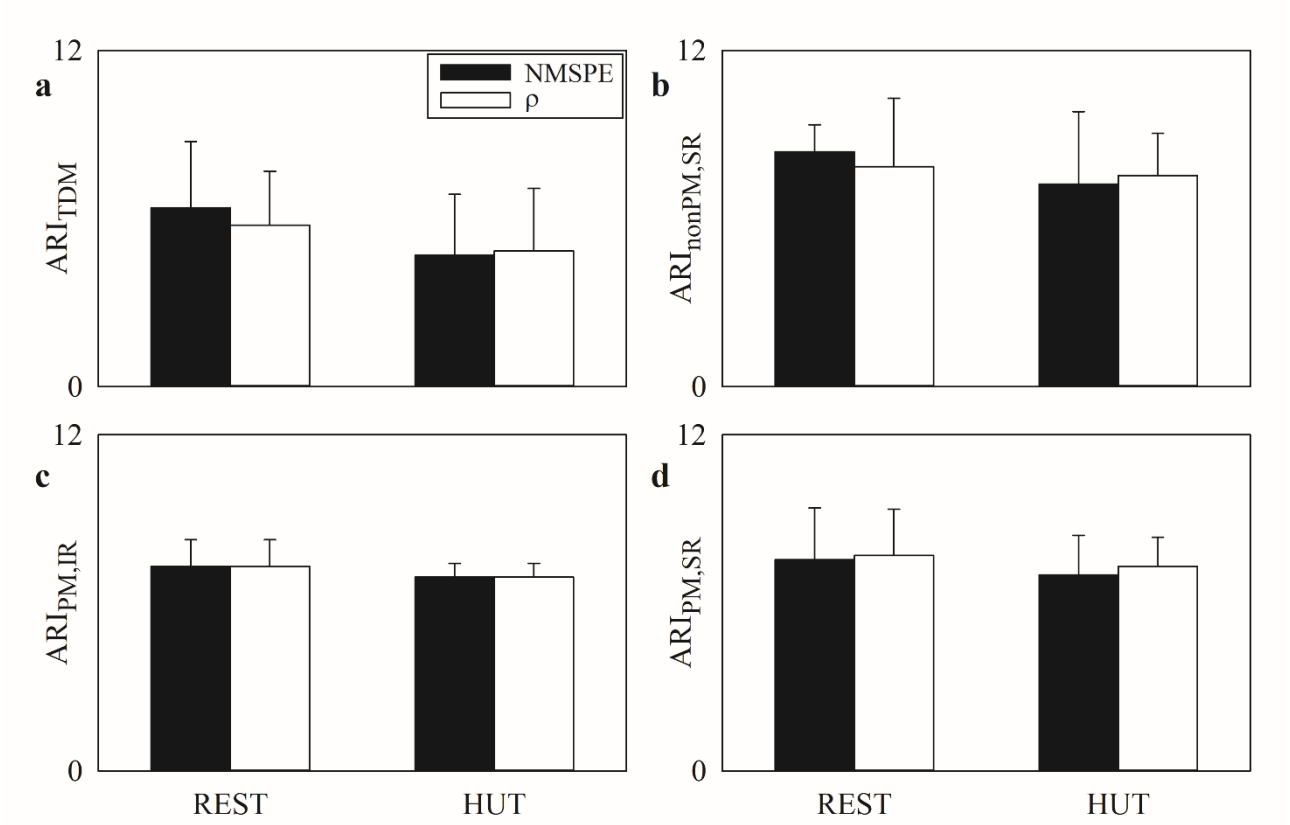
a
b
c
d
12
0
NMSPE
ρ
ARI_TDM
ARI_nonPM,SR
ARI_PM,IR
ARI_PM,SR
REST
HUT

Fig. 5

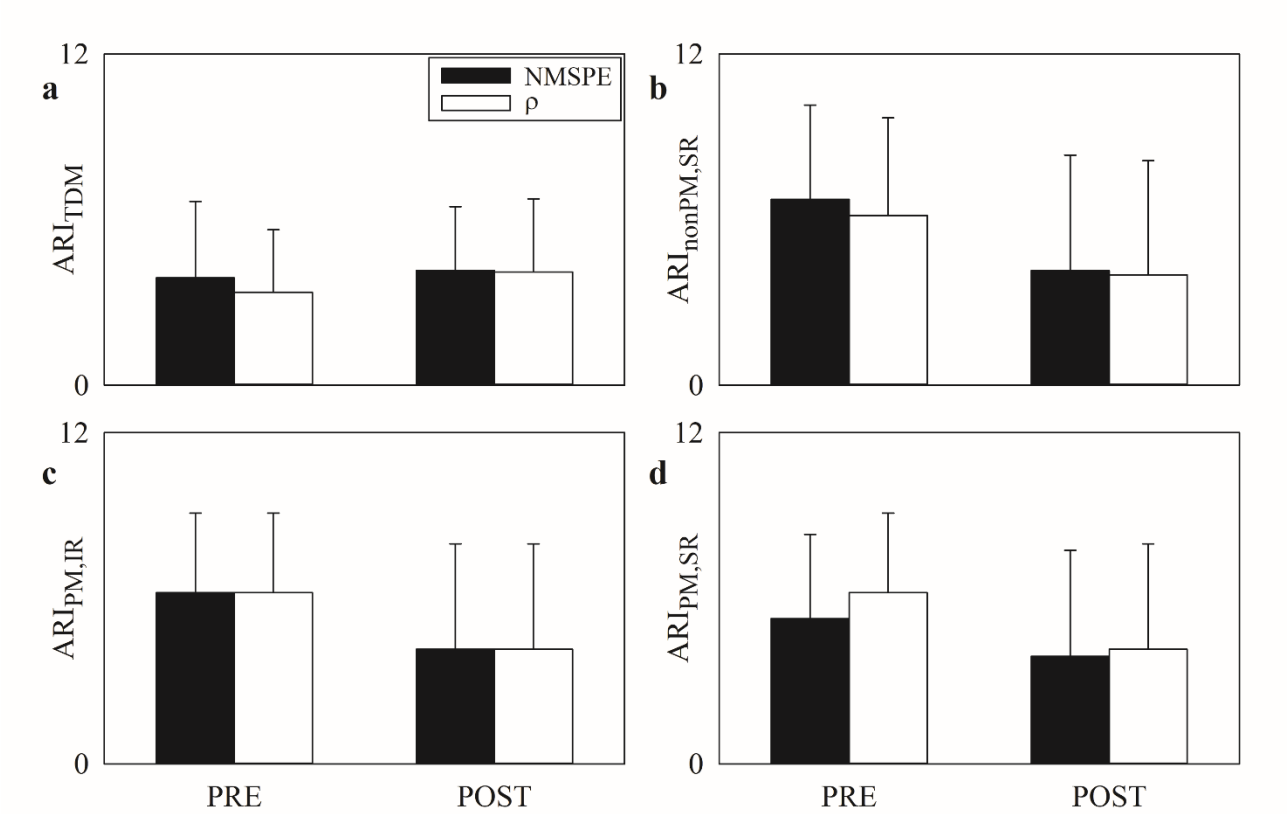

691

692 Fig. 6

693

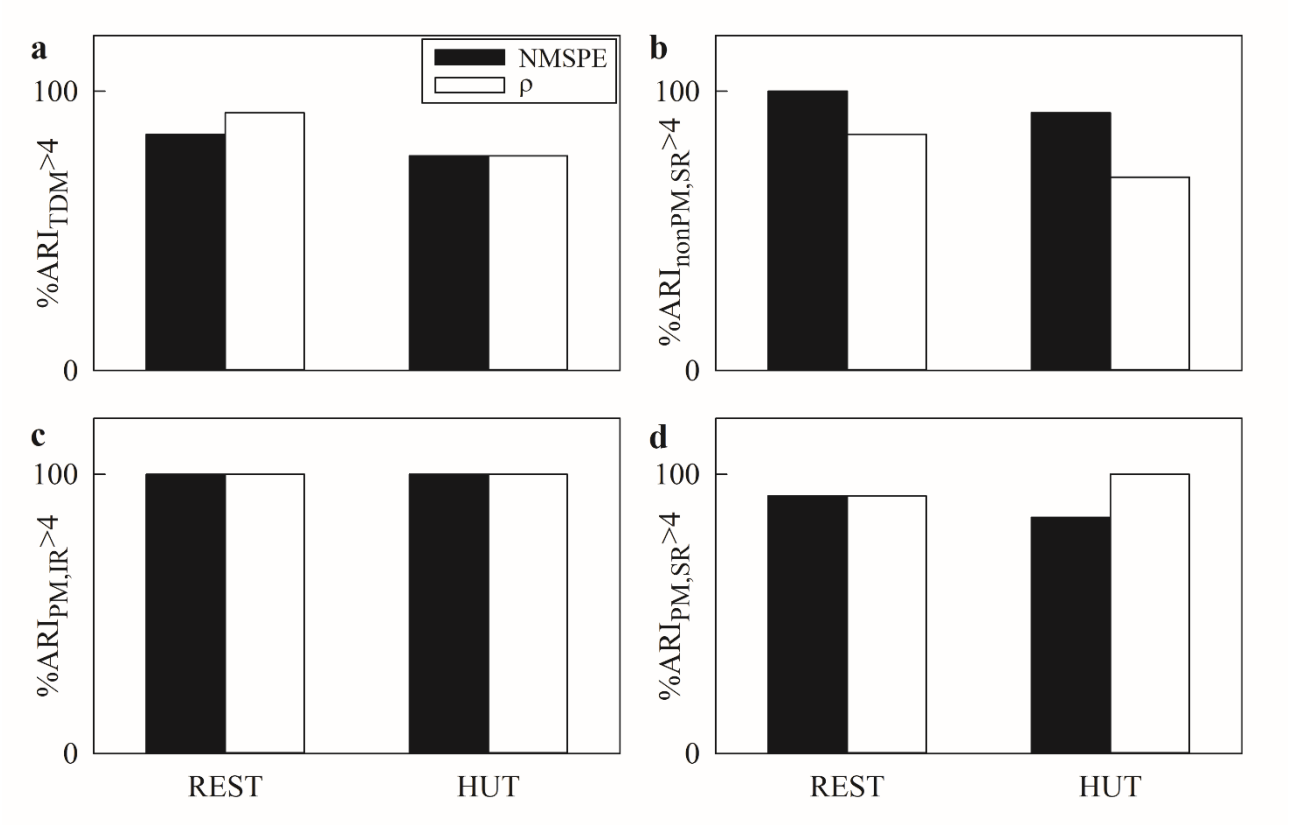
a
b
c
d
NMSPE
ρ
100
0
%ARI_TDM>4
%ARI_nonPM,SR>4
%ARI_PM,IR>4
%ARI_PM,SR>4
REST
HUT

Fig. 7

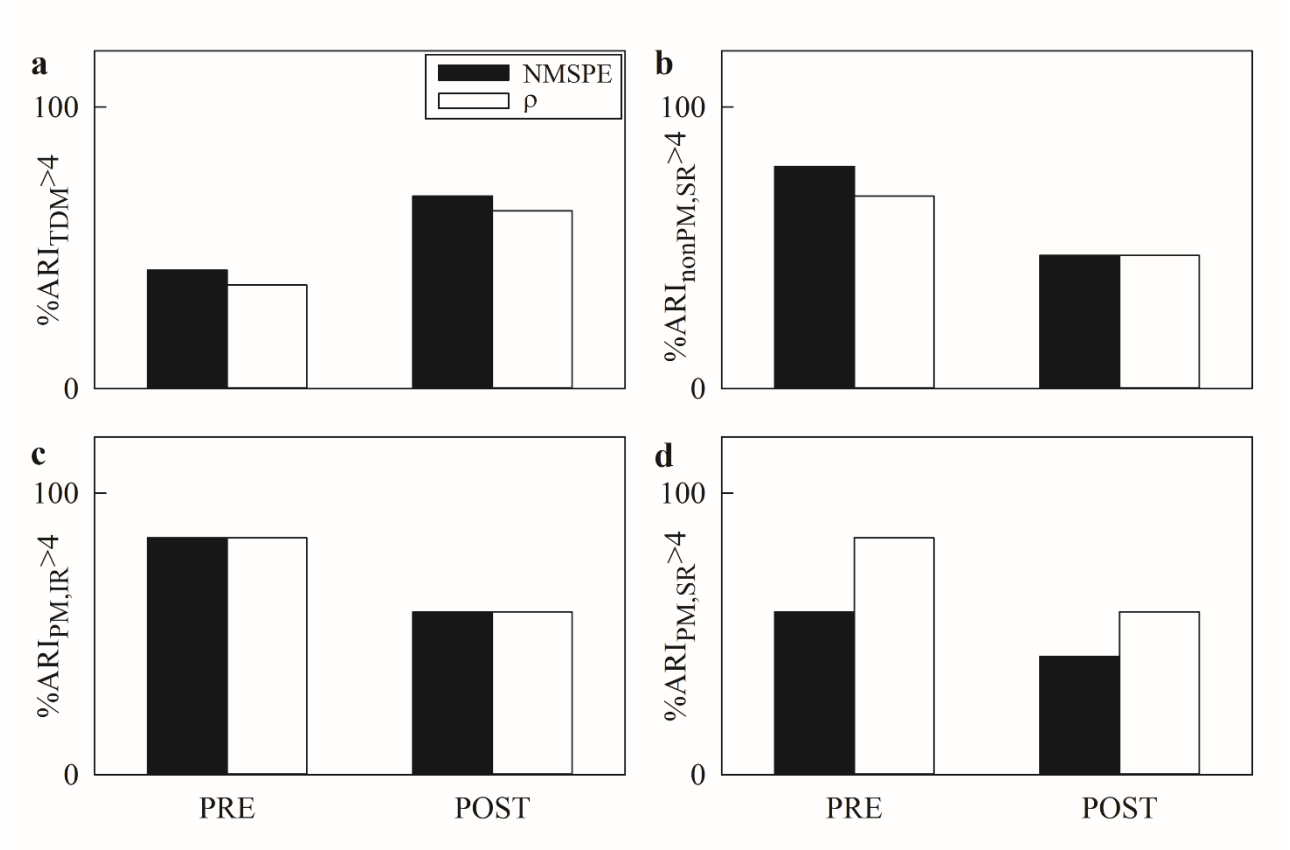
a
b
c
d
NMSPE
ρ
100
0
%ARI_TDM>4
%ARI_nonPM,SR>4
%ARI_PM,IR>4
%ARI_PM,SR>4
PRE
POST

Fig. 8

701 **Table 1.** Univariate time and frequency domain parameters in the REST-HUT protocol.

Parameter	REST	HUT
μ_{HP} [ms]	848.04 ± 188.70	672.49 ± 107.57*
σ^2_{HP} [ms^2]	2494.45 ± 2494.04	1740.67 ± 1174.15
LFa_{HP} [ms^2]	696.70 ± 575.55	1002.12 ± 1039.42
HFa_{HP} [ms^2]	710.24 ± 1019.72	207.53 ± 251.51*
μ_{MAP} [mmHg]	98.93 ± 17.19	95.23 ± 12.31
σ^2_{MAP} [mmHg^2]	20.05 ± 21.71	19.96 ± 11.36
$VLFa_{MAP}$ [mmHg^2]	5.20 ± 7.97	2.69 ± 7.87
LFa_{MAP} [mmHg^2]	4.72 ± 7.18	10.77 ± 10.42*
HFa_{MAP} [mmHg^2]	3.32 ± 5.11	1.80 ± 0.72
μ_{MCBFV} [cm·s^{-1}]	72.07 ± 23.16	61.75 ± 21.28*
σ^2_{MCBFV} [cm^2·s^{-2}]	19.17 ± 12.48	30.67 ± 25.44
$VLFa_{MCBFV}$ [cm^2·s^{-2}]	9.94 ± 14.90	12.19 ± 24.02
LFa_{MCBFV} [cm^2·s^{-2}]	2.98 ± 3.33	8.64 ± 8.09*
HFa_{MCBFV} [cm^2·s^{-2}]	0.99 ± 0.71	2.20 ± 1.20*

702 HP = heart period; MAP = mean arterial pressure; MCBFV = mean cerebral blood flow velocity;
703 LF= low frequency; VLF = very LF; HF = high frequency; μ_{HP} = HP mean; σ^2_{HP} = HP variance;
704 $LFa_{,HP}$ = HP power in LF band expressed in absolute units; $HFa_{,HP}$ = HP power in HF band
705 expressed in absolute units; μ_{MAP} = MAP mean; σ^2_{MAP} = MAP variance; $VLFa_{MAP}$ = MAP power
706 in VLF band expressed in absolute units; LFa_{MAP} = MAP power in LF band expressed in absolute
707 units; HFa_{MAP} = MAP power in HF band expressed in absolute units; μ_{MCBFV} = MCBFV mean;
708 σ^2_{MCBFV} = MCBFV variance; $VLFa_{MCBFV}$= MCBFV power in VLF band expressed in absolute
709 units; LFa_{MCBFV} = MCBFV power in LF band expressed in absolute units; HFa_{MCBFV} = MCBFV
710 power in HF band expressed in absolute units; REST = at rest in supine position; HUT = 60°
711 head-up tilt. The symbol * indicates a significant difference versus REST with $p<0.05$.
712
713

714 **Table 2.** K^2 between MAP and MCBFV in the REST-HUT protocol.

Parameter	REST	HUT
K^2_{VLF}	0.29 ± 0.16	0.36 ± 0.16*
K^2_{LF}	0.53 ± 0.21	0.72 ± 0.19*
K^2_{HF}	0.29 ± 0.16	0.42 ± 0.14*

715 MAP = mean arterial pressure; MCBFV = mean cerebral blood flow velocity; LF= low frequency;
716 VLF = very LF; HF = high frequency; K^2_{VLF} = squared coherence between MAP and MCBFV in
717 VLF band; K^2_{LF} = squared coherence between MAP and MCBFV in LF band; K^2_{HF} = squared
718 coherence between MAP and MCBFV in HF band; REST = at rest in supine position; HUT = 60°
719 head-up tilt. The symbol * indicates a significant difference versus REST with $p<0.05$.
720
721

722 **Table 3.** Univariate time and frequency domain parameters in the PRE-POST protocol.

Parameter	PRE	POST
μ_{HP} [ms]	898.62 ± 151.17	1049.20 ± 132.05*
σ^2_{HP} [ms^2]	826.66 ± 936.69	134.60 ± 106.27*
LFa_{HP} [ms^2]	105.12 ± 197.91	16.05 ± 19.14*
HFa_{HP} [ms^2]	97.96 ± 135.91	43.12 ± 66.15*
μ_{MAP} [mmHg]	99.29 ± 12.00	68.85 ± 7.84*
σ^2_{MAP} [mmHg^2]	8.67 ± 3.43	2.38 ± 1.21*
$VLFa_{MAP}$ [mmHg^2]	3.29 ± 3.33	0.09 ± 0.19*
LFa_{MAP} [mmHg^2]	0.82 ± 1.18	0.02 ± 0.02*
HFa_{MAP} [mmHg^2]	1.90 ± 3.16	1.75 ± 1.00
μ_{MCBFV} [cm·s^{-1}]	47.91 ± 16.30	37.13 ± 10.76
σ^2_{MCBFV} [cm^2·s^{-2}]	11.31 ± 10.09	4.35 ± 3.33*
$VLFa_{MCBFV}$ [cm^2·s^{-2}]	7.10 ± 10.37	0.38 ± 0.62*
LFa_{MCBFV} [cm^2·s^{-2}]	0.73 ± 0.99	1.01 ± 1.33
HFa_{MCBFV} [cm^2·s^{-2}]	0.78 ± 0.72	1.08 ± 0.93

723 HP = heart period; MAP = mean arterial pressure; MCBFV = mean cerebral blood flow velocity;
724 LF= low frequency; VLF = very LF; HF = high frequency; μ_{HP} = HP mean; σ^2_{HP} = HP variance;
725 $LFa_{,HP}$ = HP power in LF band expressed in absolute units; $HFa_{,HP}$ = HP power in HF band
726 expressed in absolute units; μ_{MAP} = MAP mean; σ^2_{MAP} = MAP variance; $VLFa_{MAP}$ = MAP power
727 in VLF band expressed in absolute units; LFa_{MAP} = MAP power in LF band expressed in absolute
728 units; HFa_{MAP} = MAP power in HF band expressed in absolute units; μ_{MCBFV} = MCBFV mean;
729 σ^2_{MCBFV} = MCBFV variance; $VLFa_{MCBFV}$= MCBFV power in VLF band expressed in absolute
730 units; LFa_{MCBFV} = MCBFV power in LF band expressed in absolute units; HFa_{MCBFV} = MCBFV
731 power in HF band expressed in absolute units; PRE = before anesthesia induction; POST = after
732 anesthesia induction. The symbol * indicates a significant difference versus PRE with $p<0.05$.
733
734

735 **Table 4.** K^2 between MAP and MCBFV in the PRE-POST protocol.

Parameter	PRE	POST
K^2_{VLF}	0.39 ± 0.19	0.13 ± 0.08*
K^2_{LF}	0.41 ± 0.18	0.14 ± 0.10*
K^2_{HF}	0.35 ± 0.19	0.20 ± 0.09*

736 MAP = mean arterial pressure; MCBFV = mean cerebral blood flow velocity; LF= low frequency;
737 VLF = very LF; HF = high frequency; K^2_{VLF} = squared coherence between MAP and MCBFV in
738 VLF band; K^2_{LF} = squared coherence between MAP and MCBFV in LF band; K^2_{HF} = squared
739 coherence between MAP and MCBFV in HF band; PRE = before anesthesia induction; POST =
740 after anesthesia induction. The symbol * indicates a significant difference versus PRE with
741 $p<0.05$.
742

Figure 1

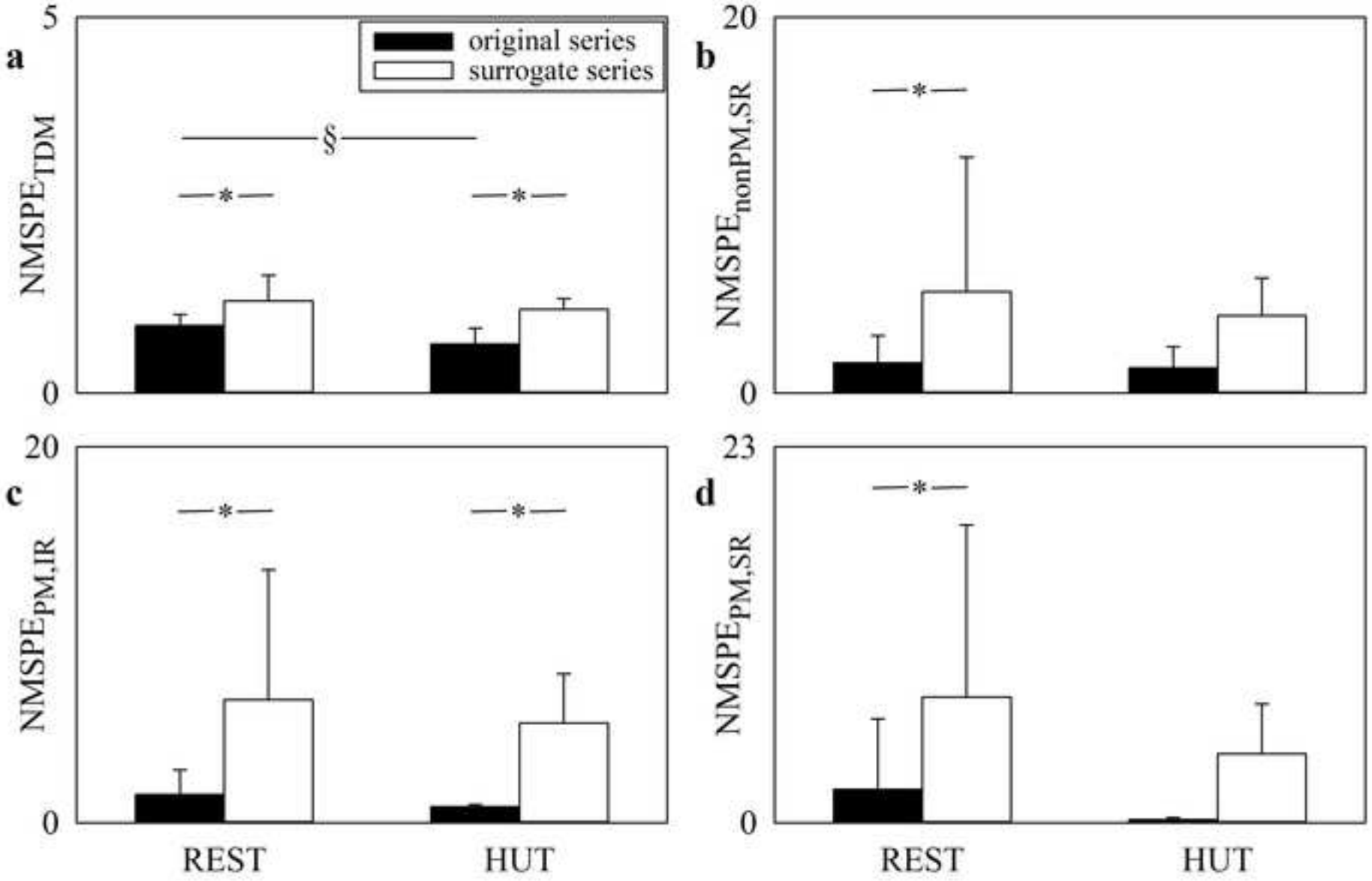

Figure 2

Click here to access/download;Figure;fig2.TIF

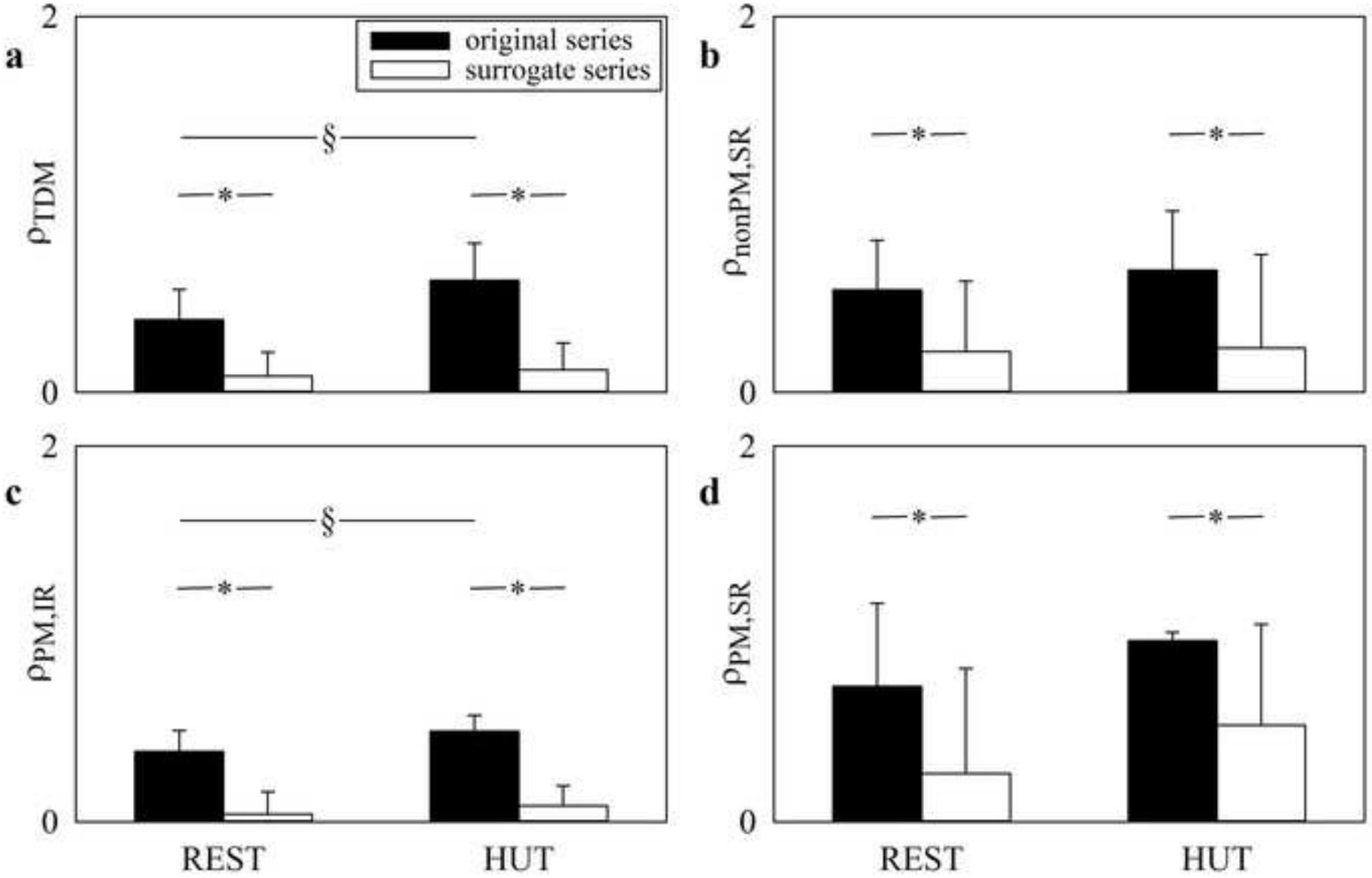

Figure 3

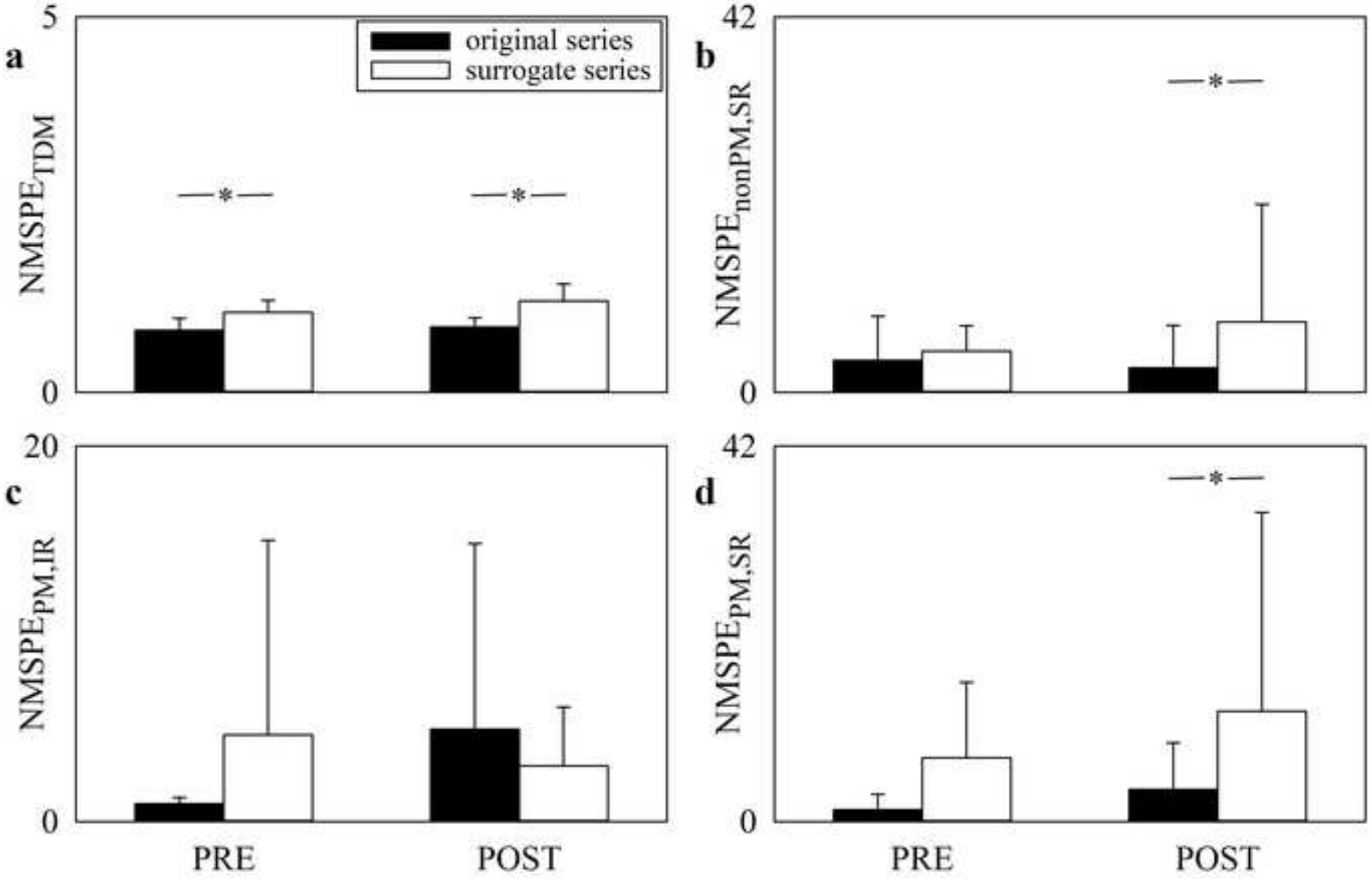

Figure 4

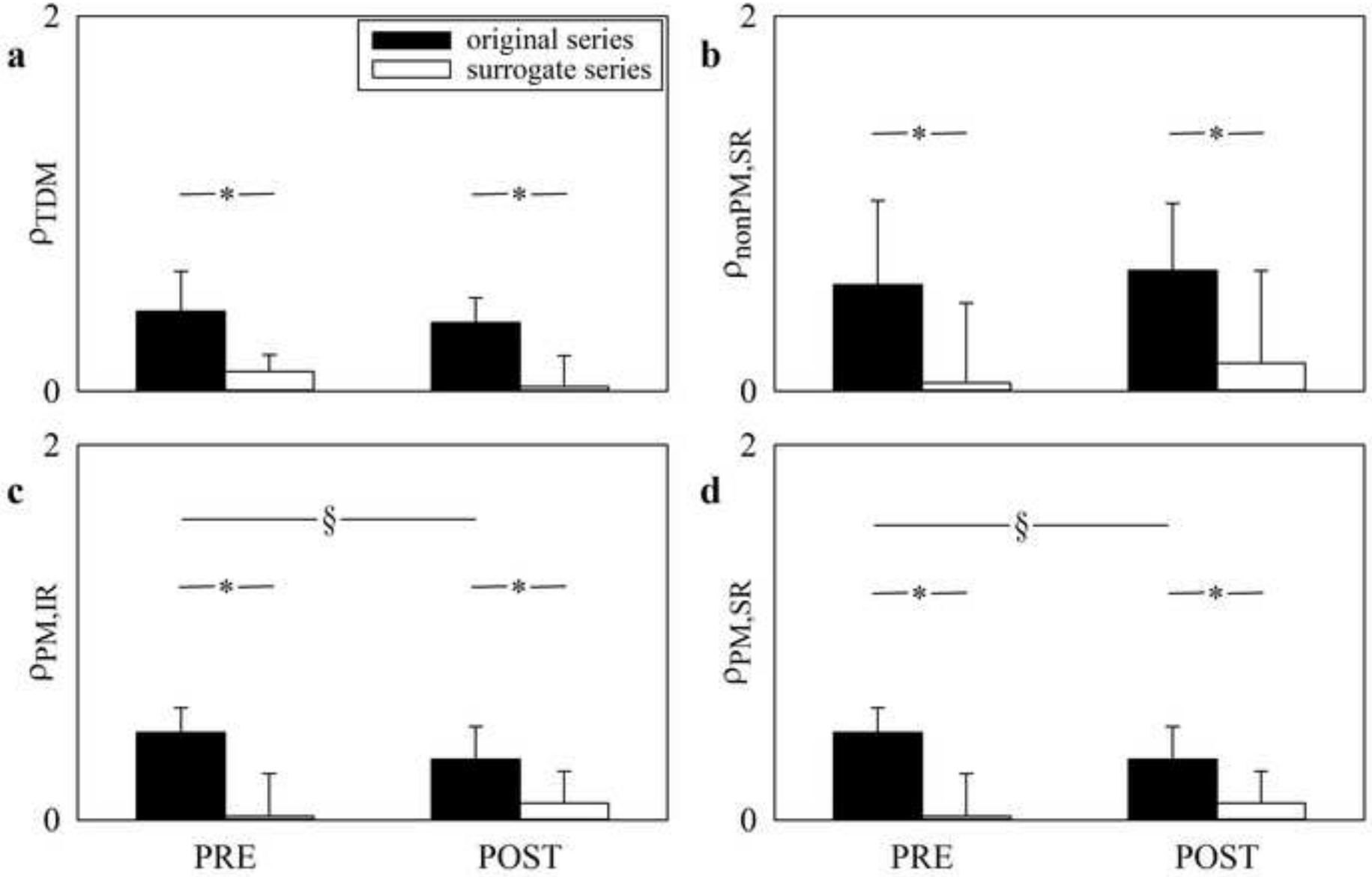

Figure 5

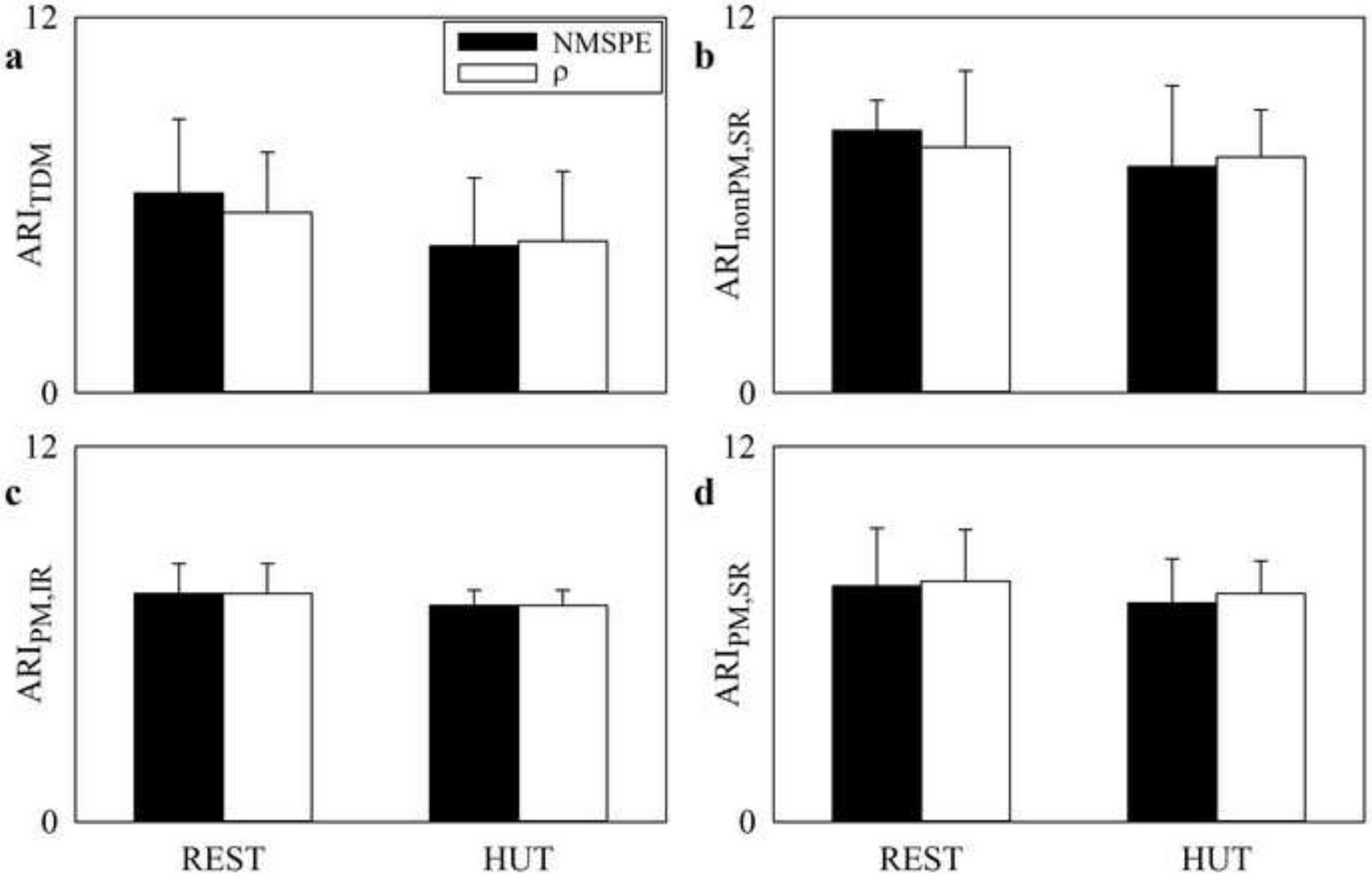

Figure 6

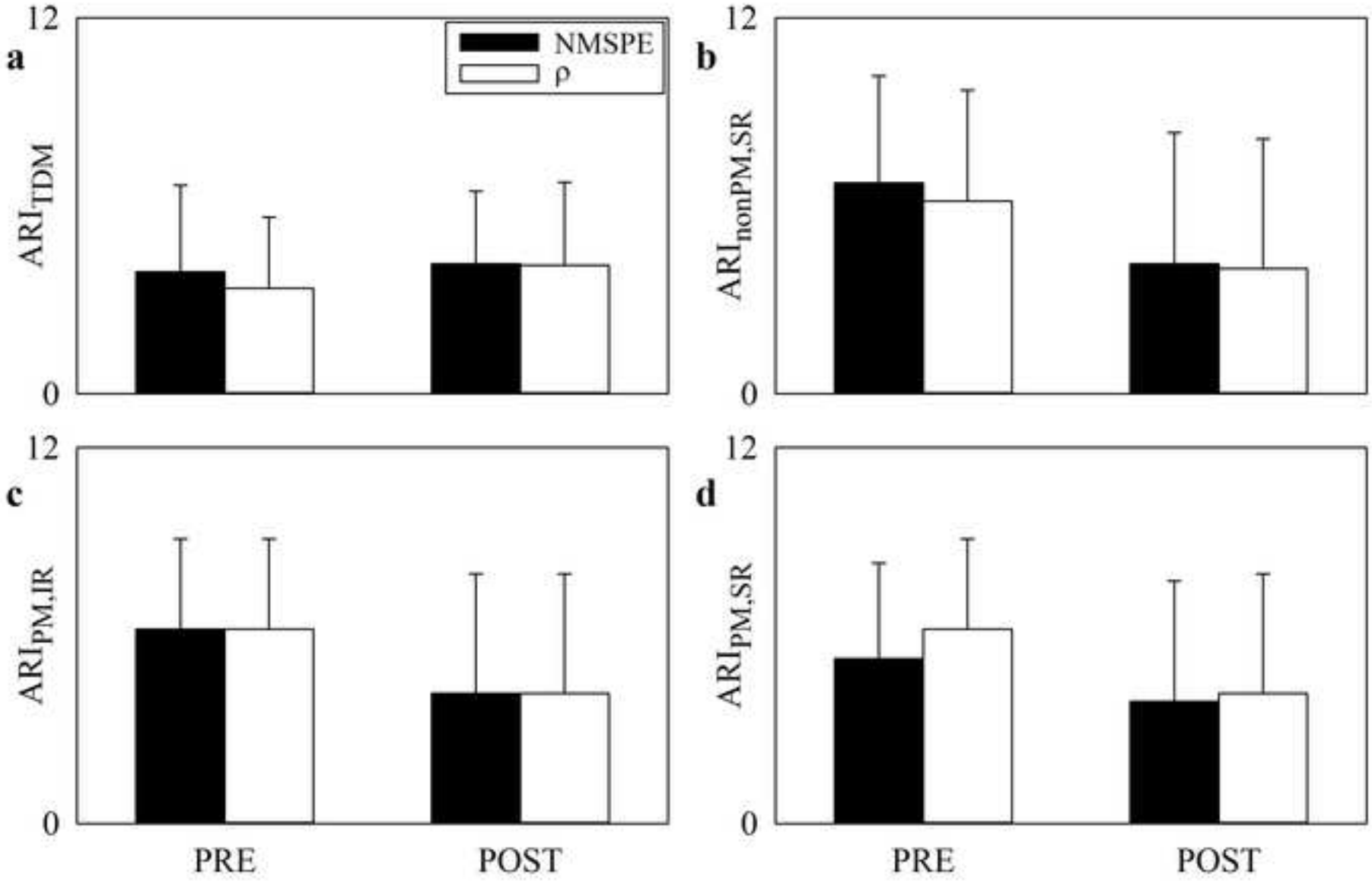

Figure 7

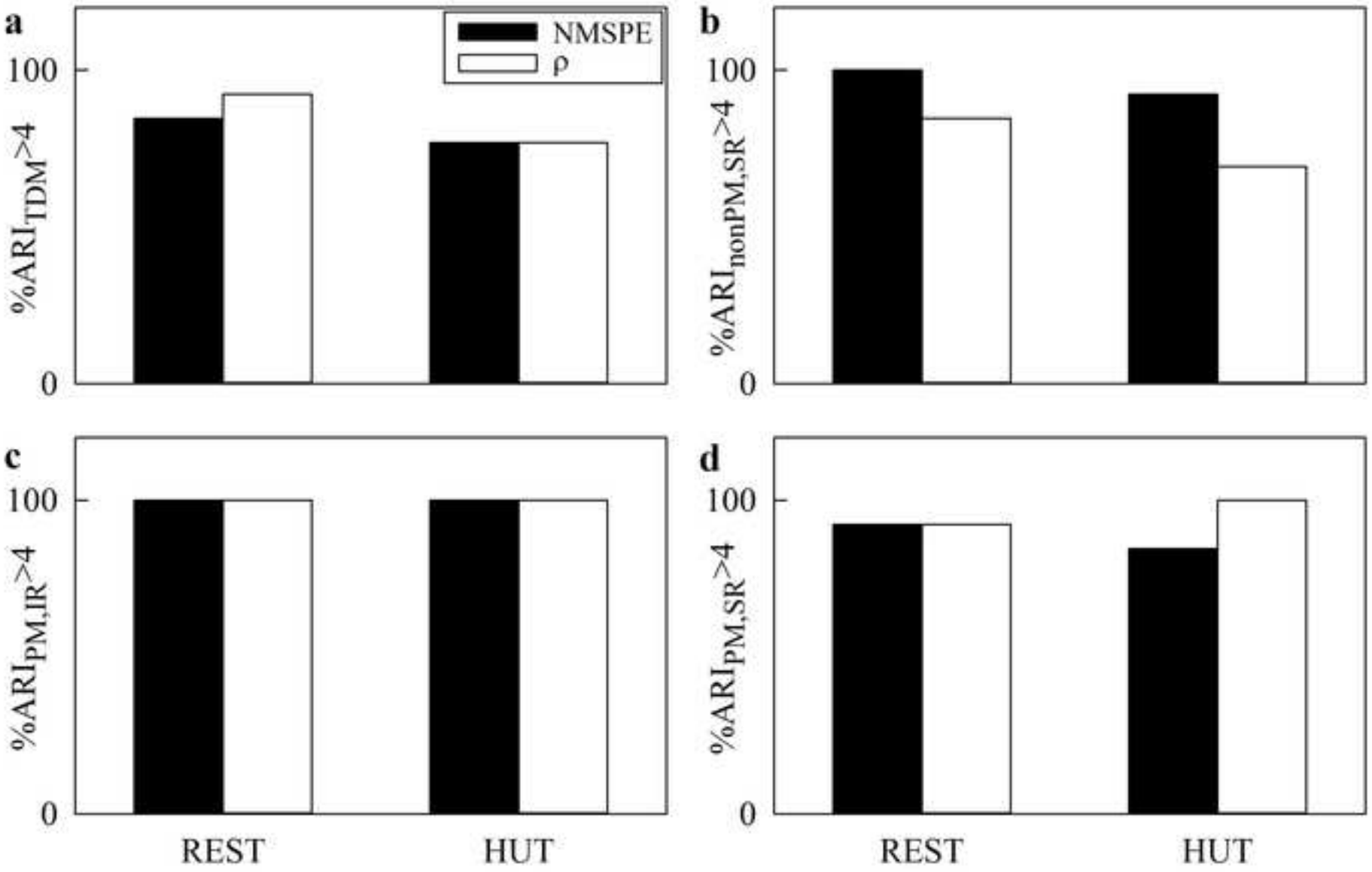

Figure 8

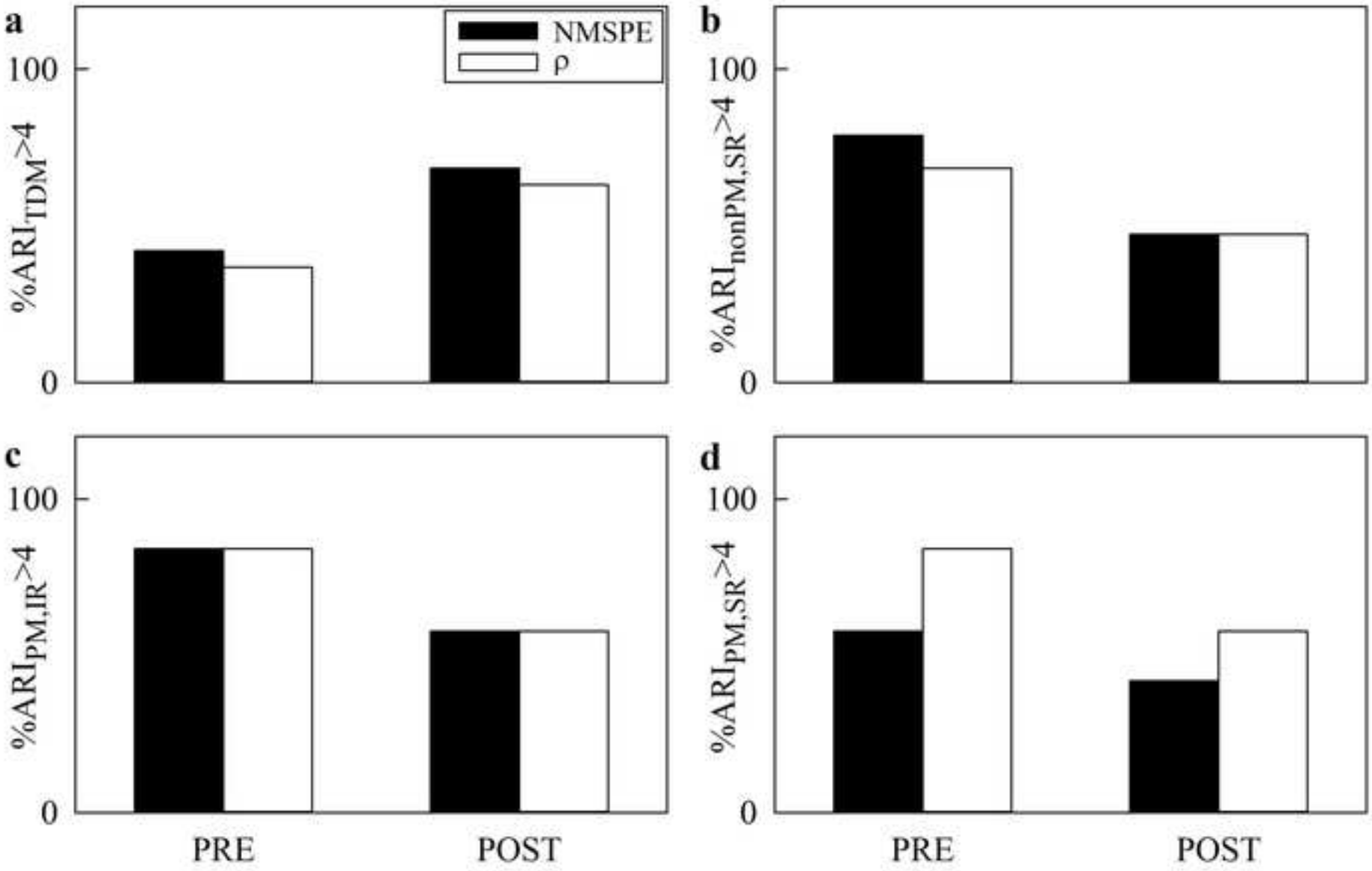

Exploring mean square prediction error and correlation metrics for the computation of the autoregulation index during propofol-based general anesthesia and head-up tilt protocols

Vlasta Bari[1], Lorenzo Barbarossa[2], Francesca Gelpi[1,3], Beatrice Cairo[3], Beatrice De Maria[4], Davide Tonon[5], Gianluca Rossato[5], Luca Faes[6], Marco Ranucci[1], Riccardo Barbieri[2], Alberto Porta[1,3]

[1]Department of Cardiothoracic, Vascular Anesthesia and Intensive Care, IRCCS Policlinico San Donato, San Donato Milanese, Milan, Italy
[2]Department of Electronics Information and Bioengineering, Politecnico di Milano, Milan, Italy
[3]Department of Biomedical Sciences for Health, University of Milan, Milan, Italy
[4]IRCCS Istituti Clinici Scientifici Maugeri, Milan, Italy
[5]Department of Neurology, IRCCS Sacro Cuore Don Calabria Hospital, Negrar, Verona, Italy
[6]Department of Engineering, University of Palermo, Palermo, Italy

Running title: Cerebral autoregulation during general anesthesia and postural challenge

Address for correspondence:

Prof. Alberto Porta, PhD
Università degli Studi di Milano
Dipartimento di Scienze Biomediche per la Salute
IRCCS Policlinico San Donato
Laboratorio di Modellistica di Sistemi Complessi
Via R. Morandi 30
20097, San Donato Milanese
Milano, Italy

Tel: +39 02 52774382
Email: alberto.porta@unimi.it